

SUPPORTING INFORMATION

Theoretical studies of a series of novel two-photon Nitric Oxide (NO)
fluorescent probes based on BODIPY

Li Zhang,¹ Lu-Yi Zou,¹ Jing-Fu Guo,² Dan Wang,¹ Ai-Min Ren*

¹State Key Laboratory of Theoretical and Computational Chemistry,

Institute of Theoretical Chemistry, Jilin University,

Changchun 130061, People's Republic of China

²School of Physics, Northeast Normal University, 130024, P. R. China

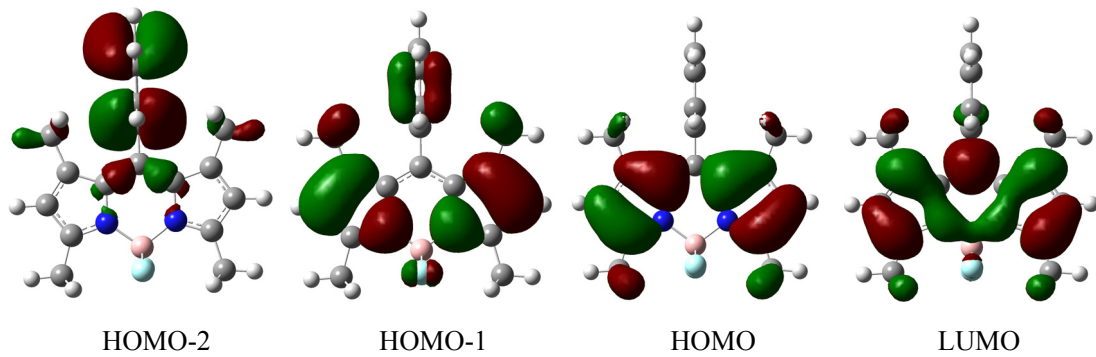
*Corresponding author: Tel./fax: +86-431-88498567 (A. M. Ren)

E-mail addresses: aimin_ren@yahoo.com

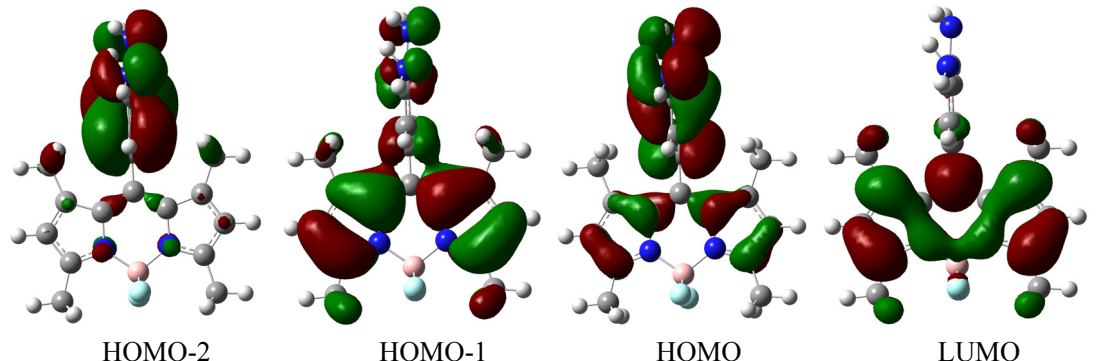
Section S1 The mainly related frontier molecular orbitals.

On the basis of the optimized molecular geometries, we calculated the OPA spectra (UV-Vis spectra) for all molecules in this work by means of the TDDFT//CAM-B3LYP/6-31G(d) approach with the SMD model. Furthermore, in order to gain a deeper insight into the intramolecular charge transfer, the mainly related frontier molecular orbitals (FMO) are all illustrated in Fig.S1 as follows.

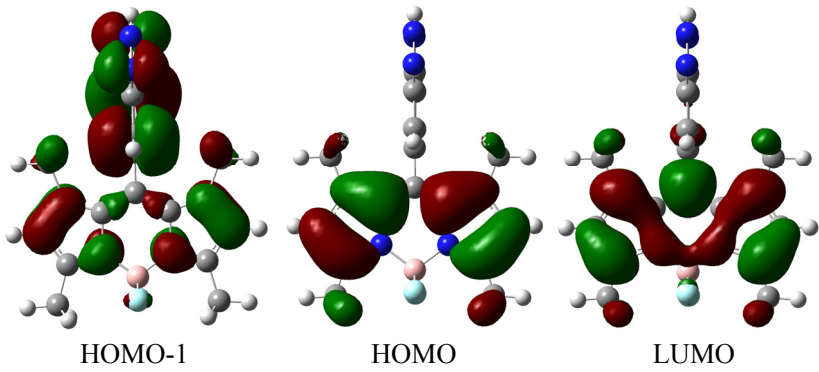
BODIPY-1



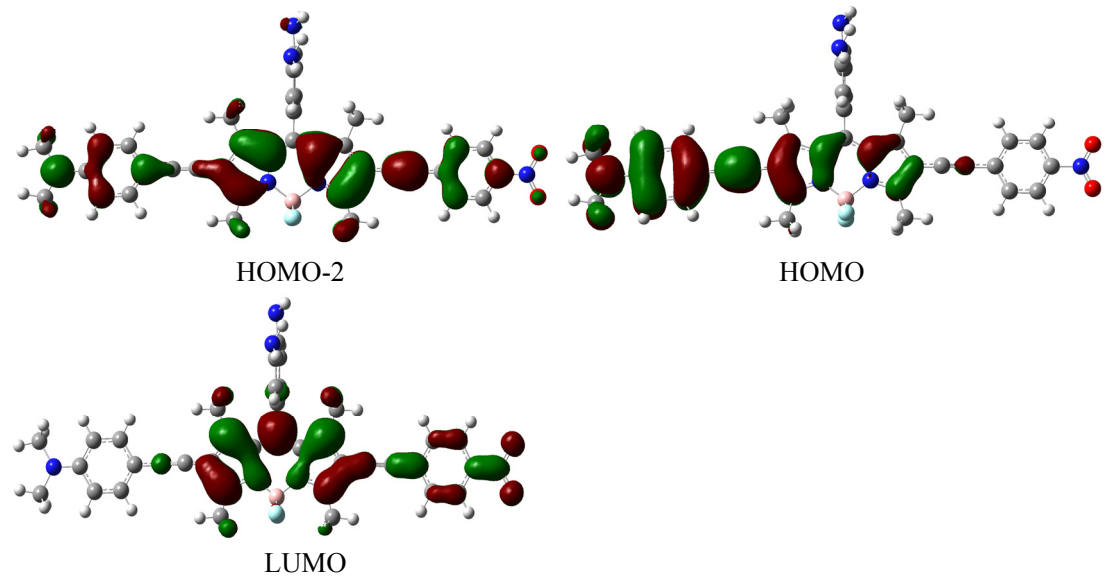
DAMBO



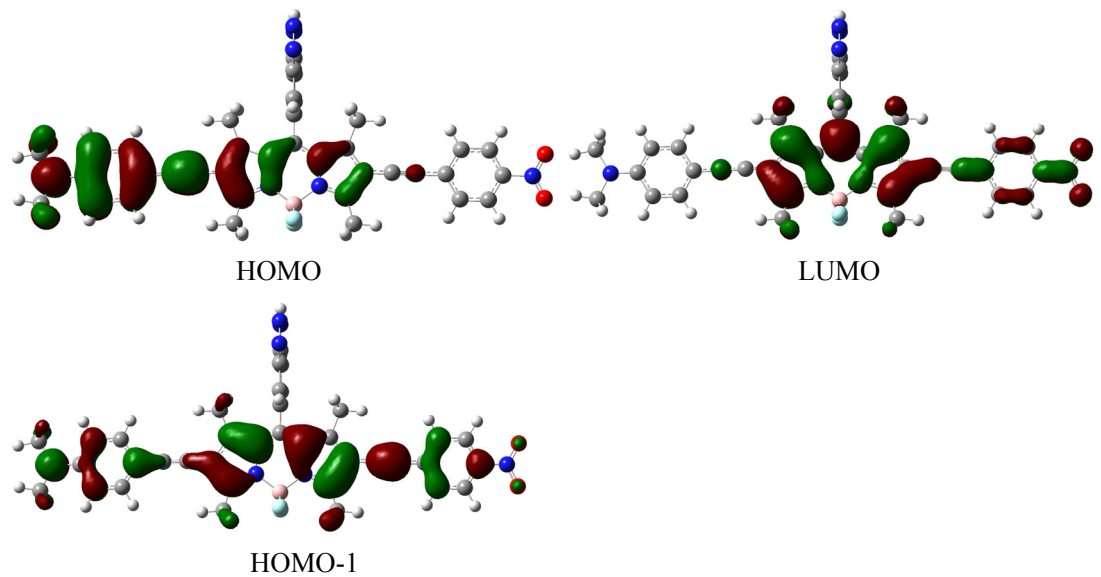
DAMBO-T



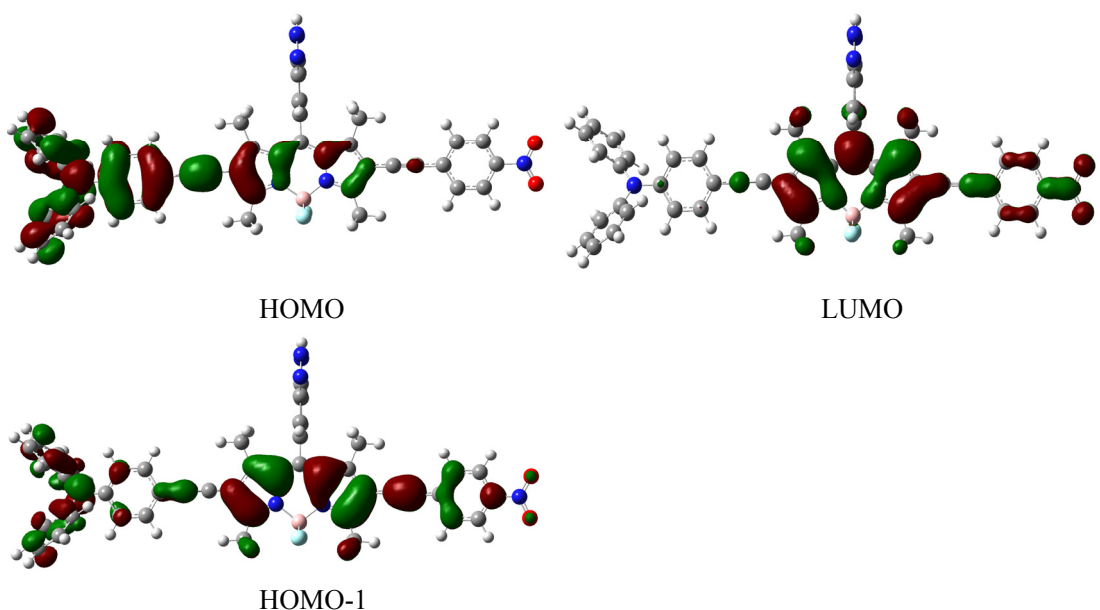
D1



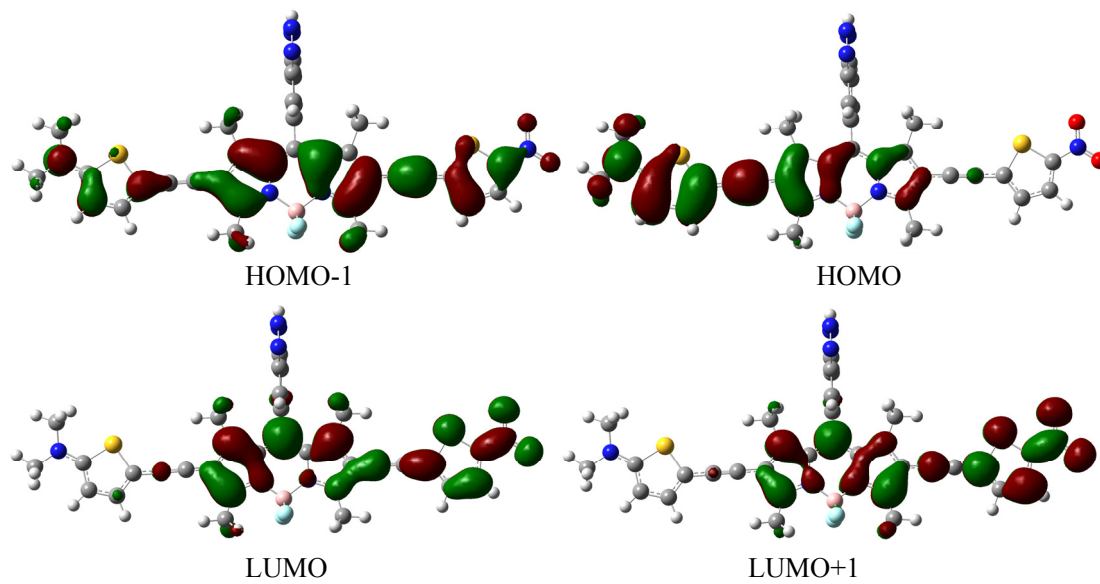
D1-T



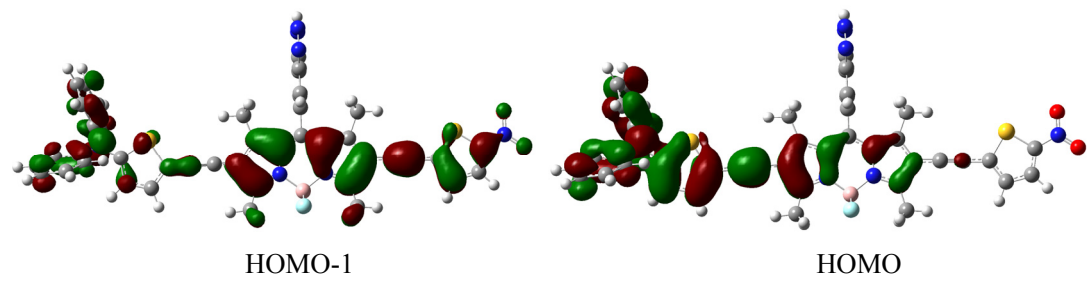
D2-T

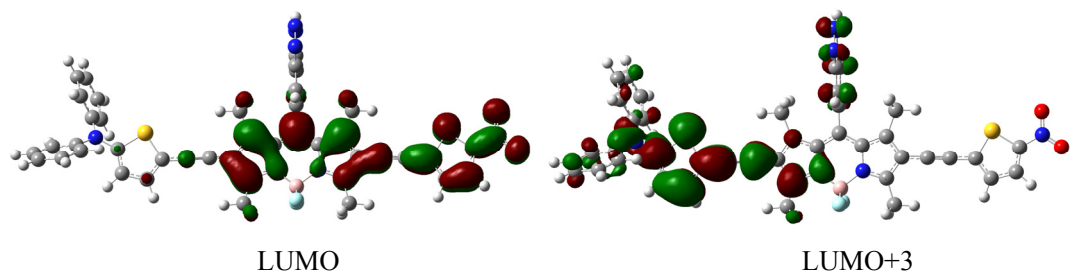


D3-T

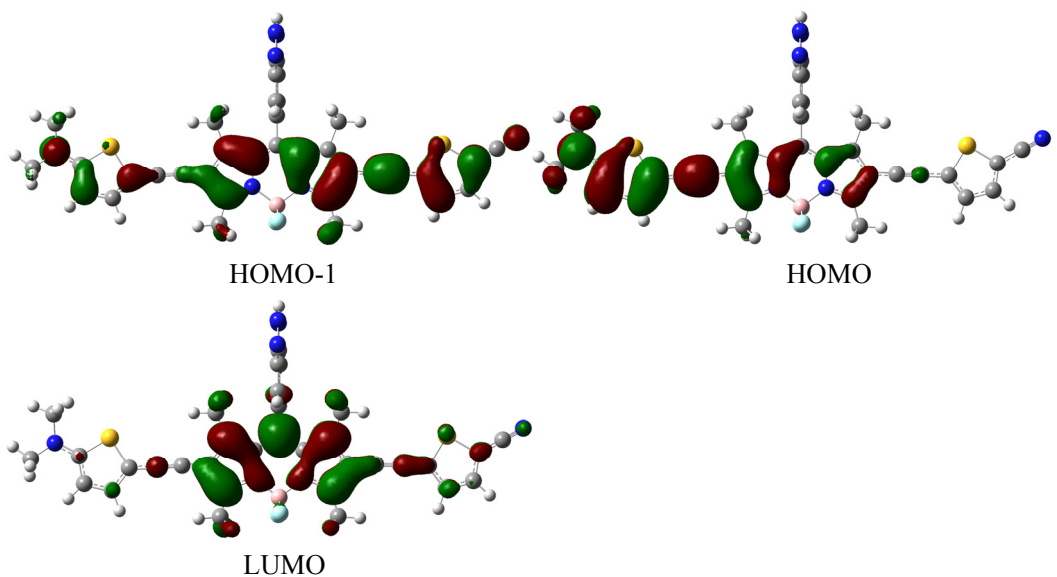


D4-T

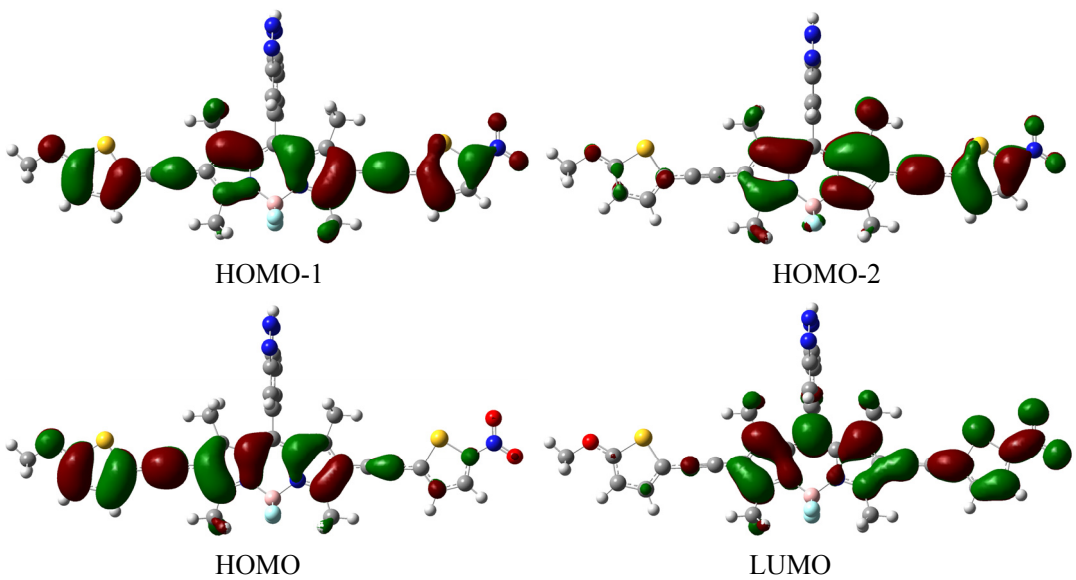


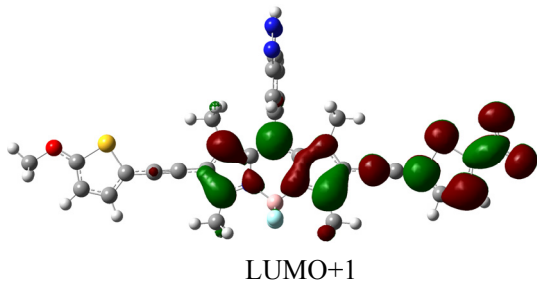


D5-T



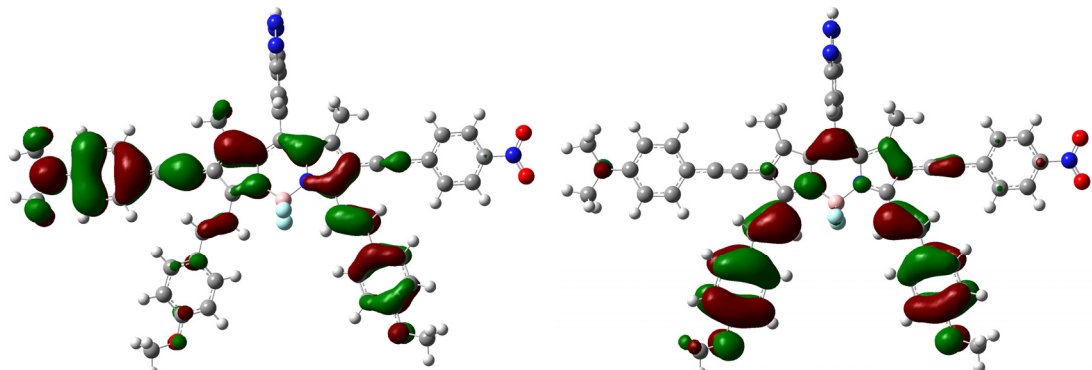
D6-T





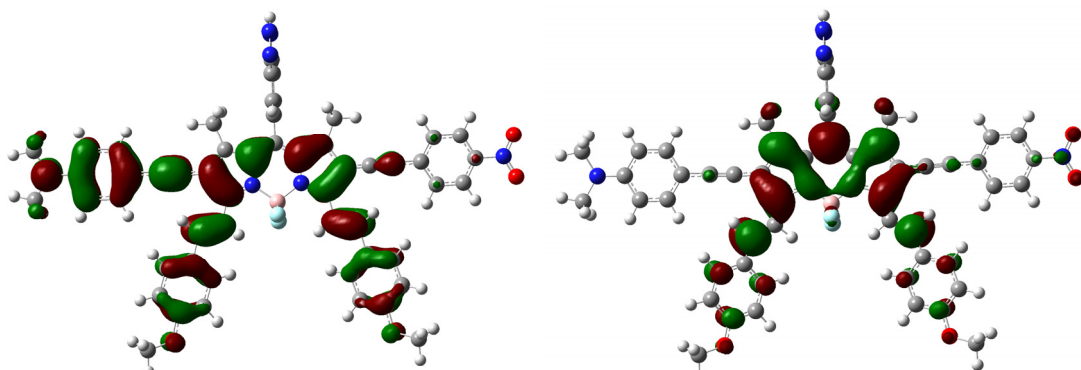
LUMO+1

D7-T



HOMO-1

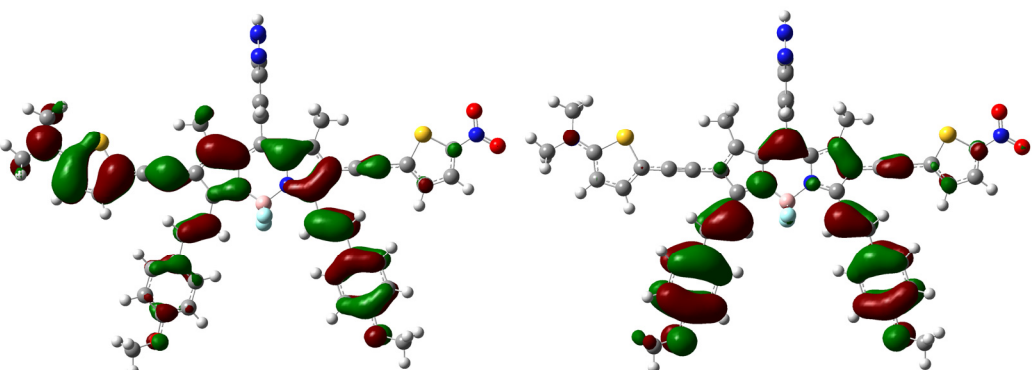
HOMO-2



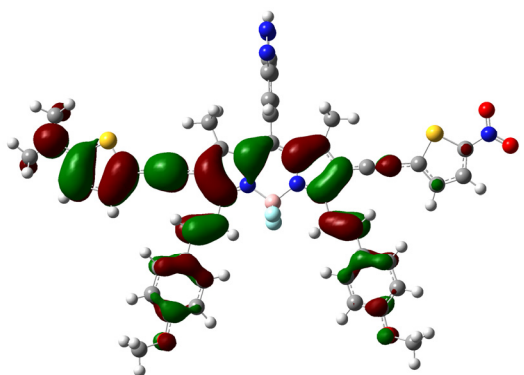
HOMO

LUMO

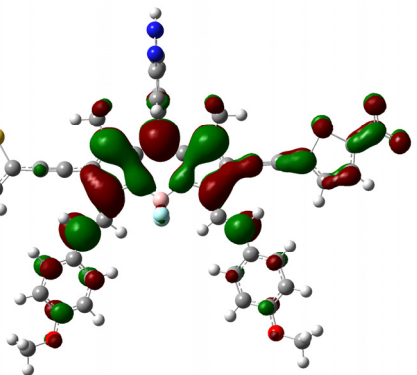
D8-T



HOMO-1

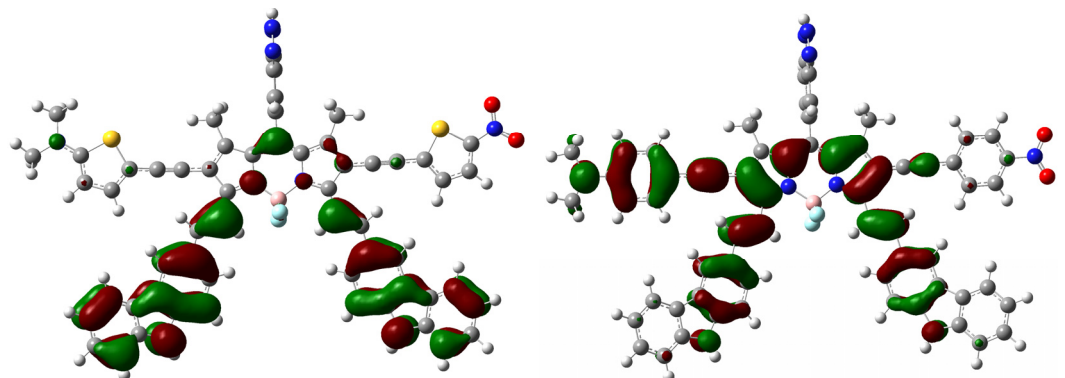


HOMO-2

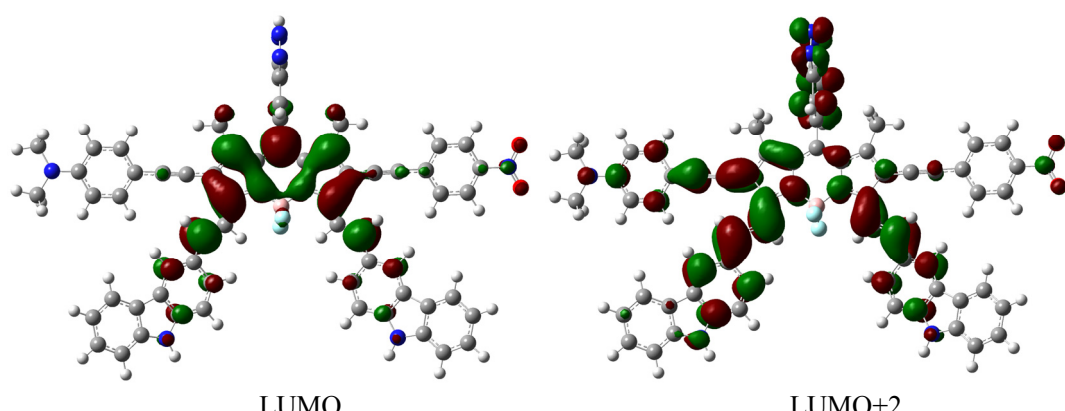


HOMO

D9-T

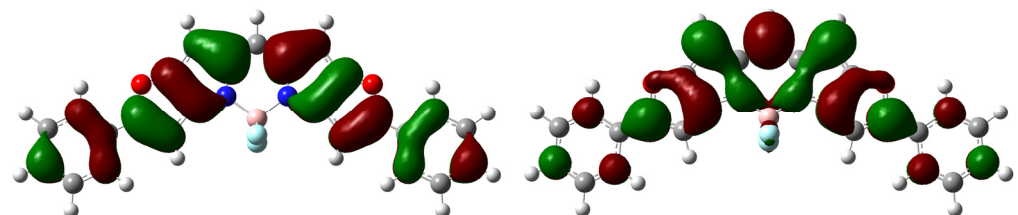


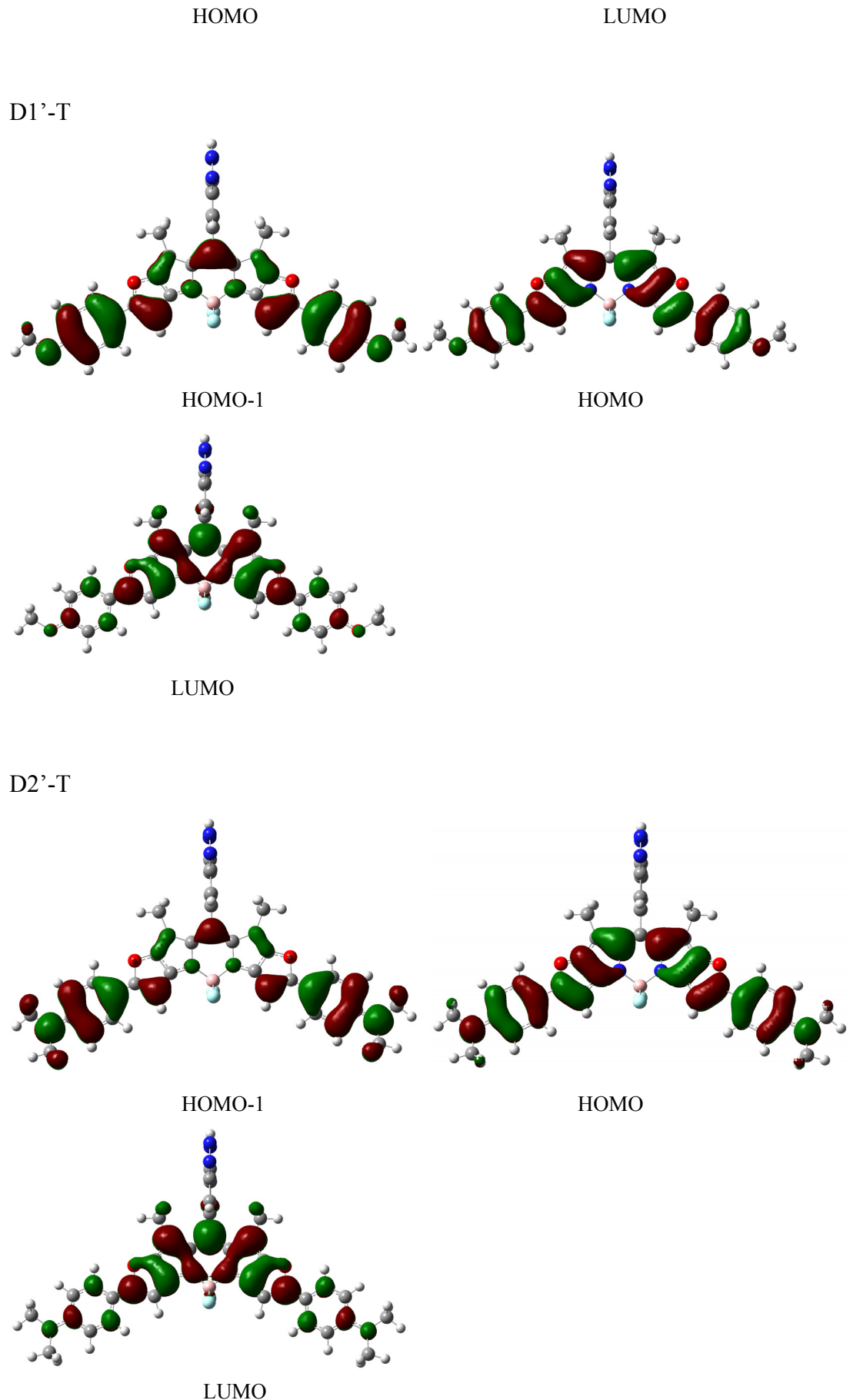
HOMO-2



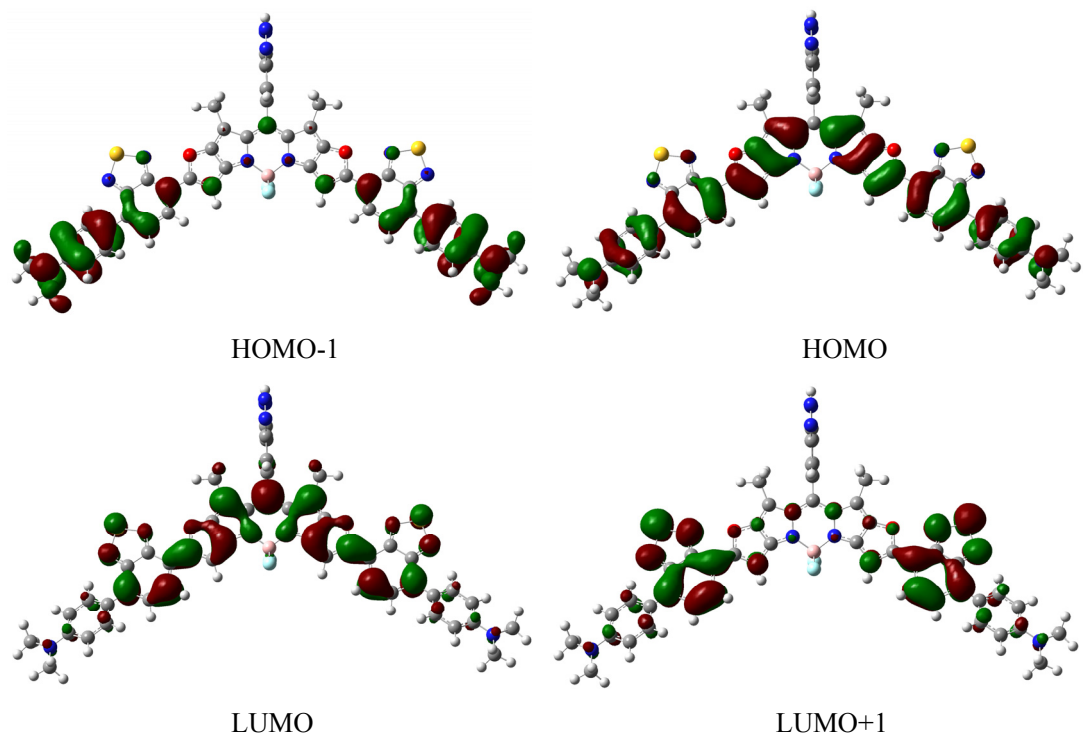
LUMO+2

KFL-5

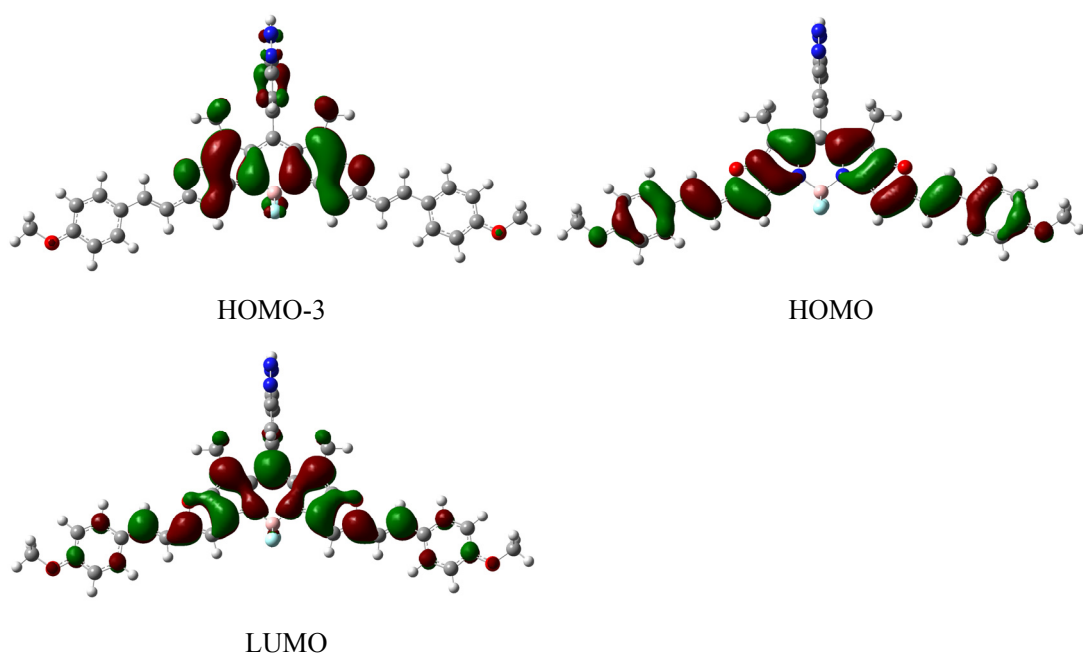




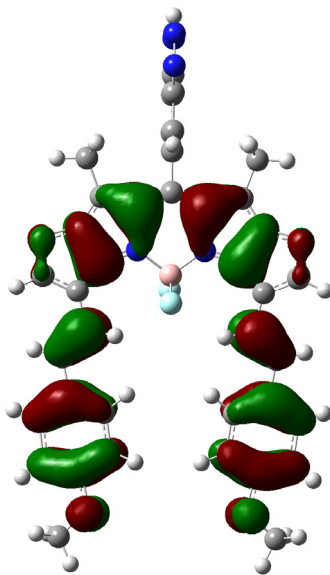
D3'-T



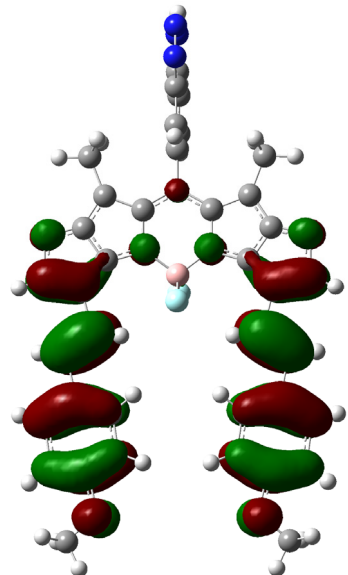
D4'-T



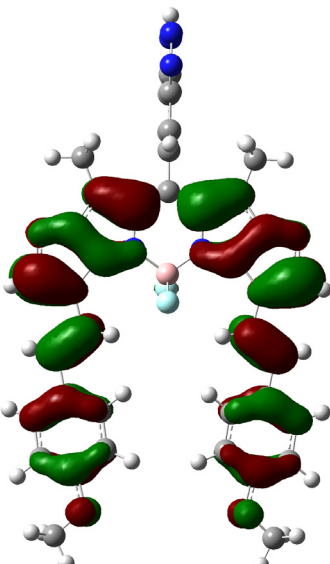
D5'-T



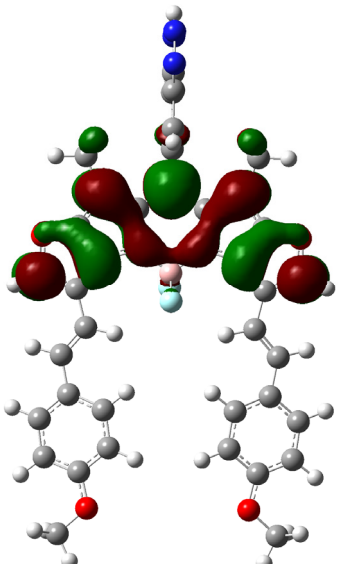
HOMO-2



HOMO-1

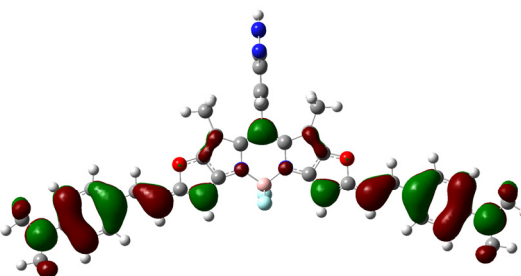


HOMO

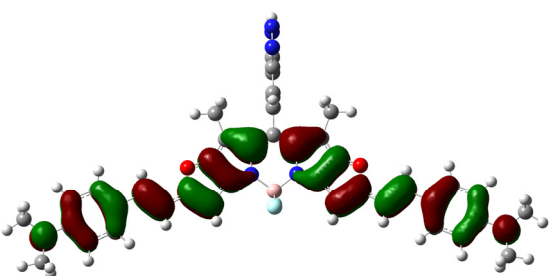


LUMO

D6'-T



HOMO-1



HOMO

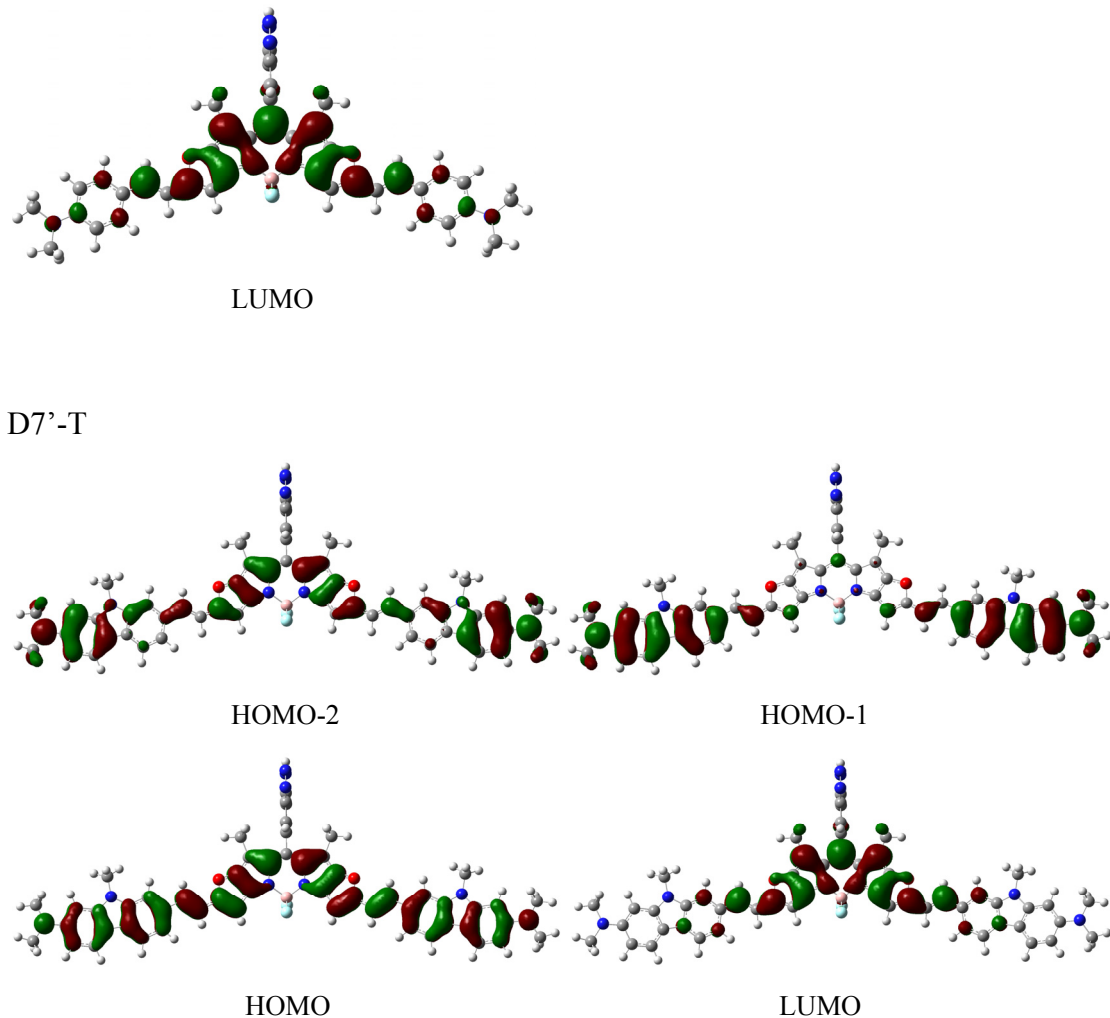
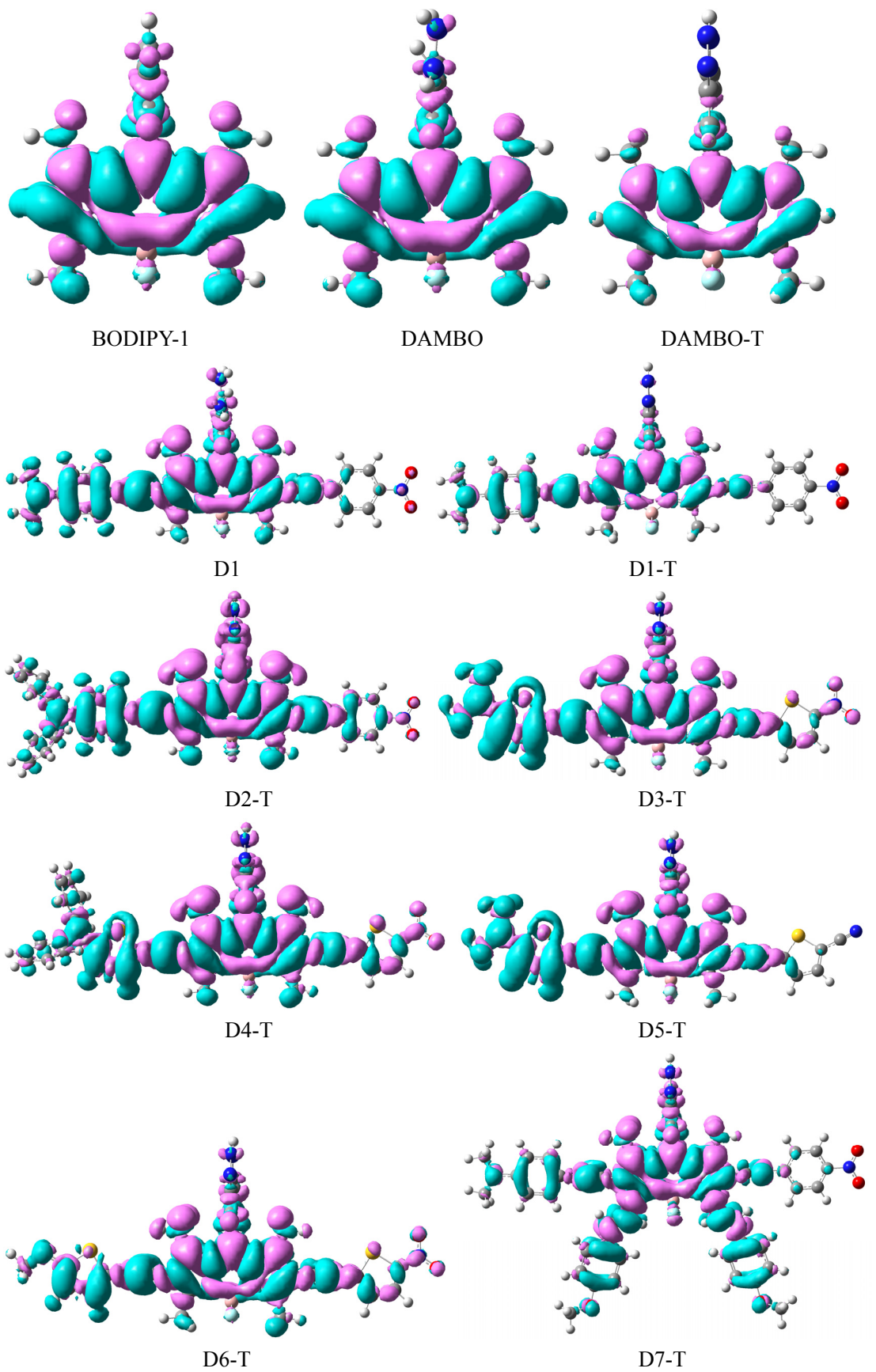
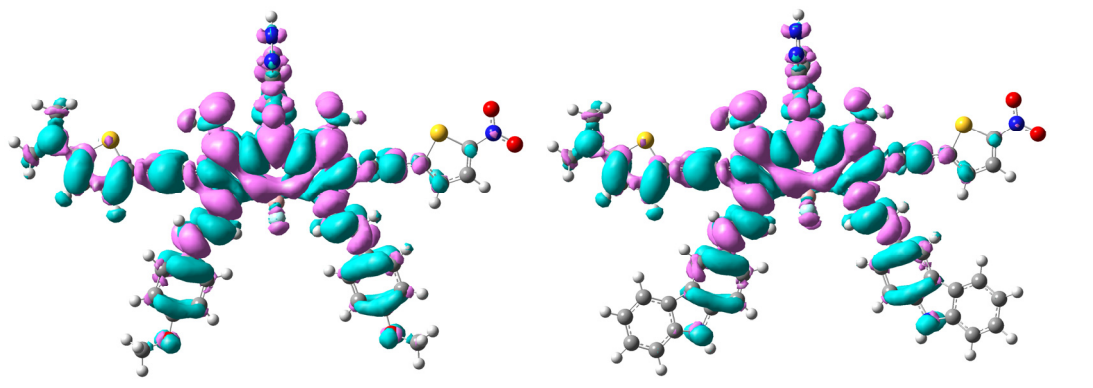


Fig.S1. Contour surfaces of all main orbitals for all of the molecules studied on the ground structures.

Section S2. The density difference plots of all studied molecules.

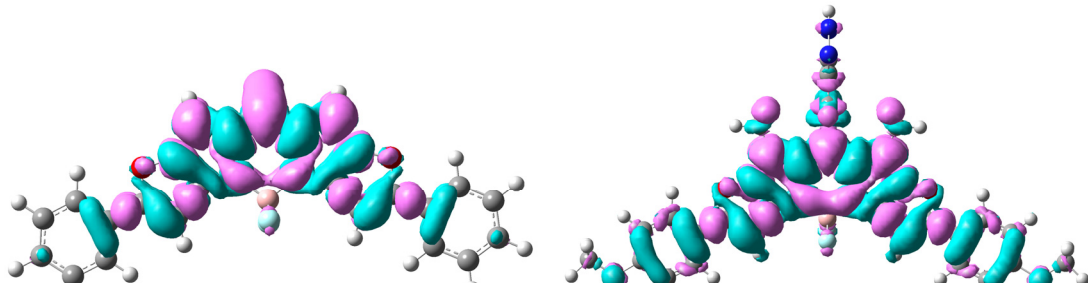
Moreover, to make clear the process of the charge transfer resulting from electronic transition, as well as how the charge transfer influences on the features of OPA and TPA, the density difference plots of all studied molecules have been drawn in Fig.S2.





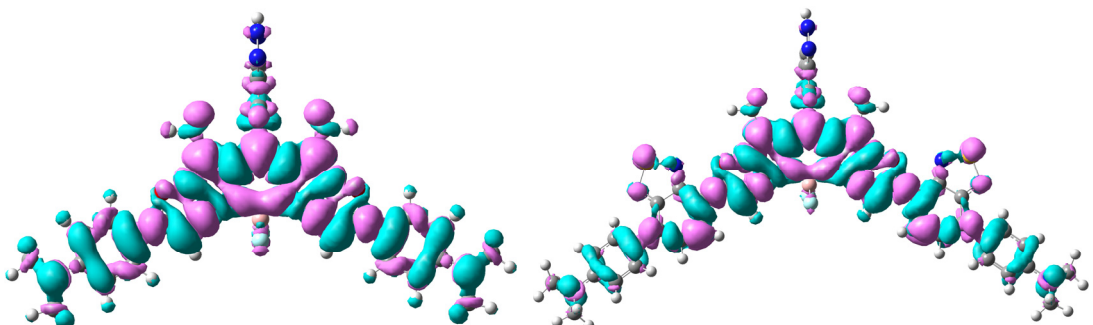
D8-T

D9-T



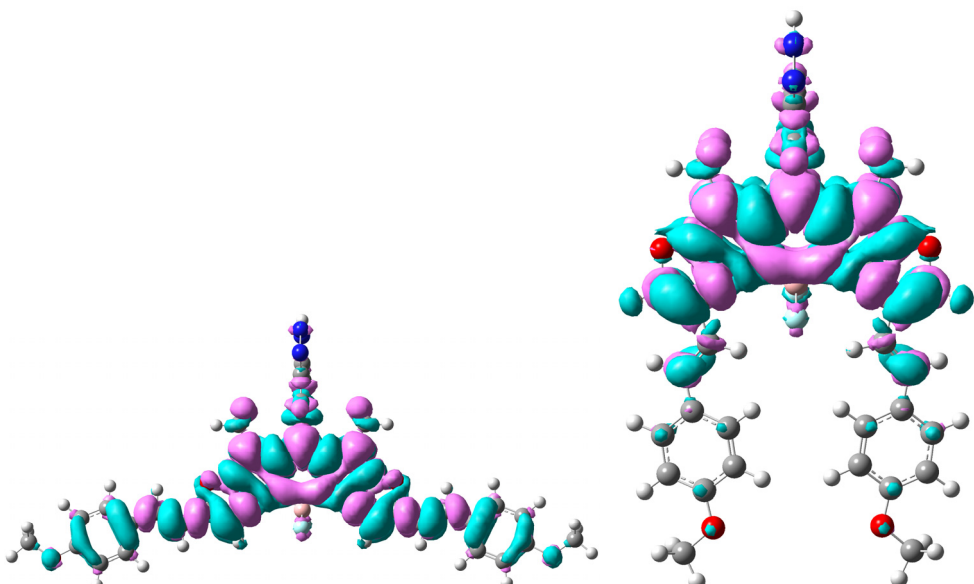
115

D1'-T



D2'-T

D3'-T



D4'-T

D5'-T

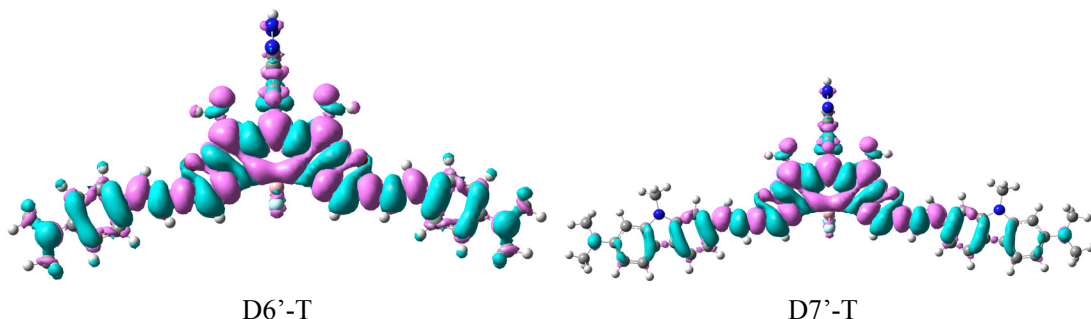


Fig.S2. Plots of the density difference between the GS and the ES calculated for the system.

Section S3 The calculations on the excited states of related studied molecules

Moreover, the dark state can be used to verify the fluorescence-OFF feature of the probes, however, such approach is not fully applicable for the NO probes in this study, and the calculated results of excited states for the studied NO probes and the corresponding reaction products performed at TDDFT//B3LYP/6-31G(d) level are listed in Table S1, including the excitation energy, the composition, oscillator strength (f) and the configuration interaction (CI) coefficient of the wavefunction for each excitation. In addition, we have carefully checked the dark states in our NO probes using the approach applied to RSH probes (Org. Biomol. Chem., 2011, 9, 3844–3853). Although our reproduced results show that the fluorescence-OFF feature can be verified by the dark state for the RSH probes, the ‘states’ approach is not fully applicable to NO probes. The reasons should be attributed to the dependence of the ‘states’ approach on the selection of functionals and the specific system of probes:

1. The ‘states’ approach is extremely dependent on the applied functionals: the dark state can be observed for B3LYP but not for CAM-B3LYP (see Tables S2-S3). We have perfectly reproduced the results of excited states for Probe 1, BODIPY1, Probe 2

and BODIPY2 in literature “*Org. Biomol. Chem.*, 2011, 9, 3844–3853” using B3LYP functional (see Table S2). However, when we calculate the excited states of these probes using CAM-B3LYP functional, the dark state feature vanishes (see Table S3). The same trend also occurs in molecules DAMBO and DAMBO-T studied in our work (see Tables S2-S3). Because the one- and two-photon absorption results obtained by CAM-B3LYP functional are in better agreement with the experiments than B3LYP, we choose CAM-B3LYP to carry out our study, which is not suitable for the calculation of dark state;

2. We also find that the ‘states’ approach is highly dependent on the kind of probes: it is applicable for RSH probes but not fully feasible for other probes, no matter with B3LYP or CAM-B3LYP functional. A typical example is one of the BODIPY derivatives, HK-Green-2 (*Org. Lett.*, 2009, 11, 1887–1890), its PET feature can be verified only by orbitals rather than dark state (see Table S4). The most of NO probes in our present study share similar structure-property relations with HK-Green-2 (see Fig.1, Table S1 and Table S4). Some PET probes with non-BODIPY structures have also been listed in Table S4 and one can find the dark state approach is not applicable. Even though some probes in our work do not display dark state at TDDFT//B3LYP/6-31G(d) level, the PET process still can be verified by orbitals, for example, D5 and D5-T, D7' and D7'-T respectively (more details see **Section S4**).

Table S1 Calculated results of the studied molecules at TDDFT//B3LYP/6-31G(d) level

Compounds	Electronic transitions	Excitation energy	f	Composition	CI
-----------	------------------------	-------------------	---	-------------	----

D1	$S_0 \rightarrow S_1$	1.75 eV (707.65 nm)	0.7672	H→L	0.67403
	$S_0 \rightarrow S_5$	2.41 eV (513.90 nm)	1.0411	H-2→L	0.68554
D1-T	$S_0 \rightarrow S_1$	1.71 eV (723.94 nm)	0.7765	H→L	0.69001
	$S_0 \rightarrow S_3$	2.39 eV (518.33 nm)	1.0469	H-1→L	0.69546
D2	$S_0 \rightarrow S_1$	1.84 eV (673.17 nm)	0.8065	H→L	0.67790
	$S_0 \rightarrow S_4$	2.41 eV (523.74 nm)	0.9939	H-2→L	0.66842
D2-T	$S_0 \rightarrow S_1$	1.79 eV (691.65 nm)	0.7858	H→L	0.68799
	$S_0 \rightarrow S_3$	2.34 eV (529.96 nm)	1.0327	H-1→L	0.68951
D3	$S_0 \rightarrow S_1$	1.55 eV (798.39 nm)	0.7458	H→L	0.66980
	$S_0 \rightarrow S_5$	2.32 eV (534.51 nm)	1.1316	H-2→L	0.68009
D3-T	$S_0 \rightarrow S_1$	1.51 eV (818.68 nm)	0.7715	H→L	0.67425
	$S_0 \rightarrow S_5$	2.30 eV (538.83 nm)	1.2039	H-1→L	0.69046
D4	$S_0 \rightarrow S_1$	1.72 eV (722.08 nm)	0.7824	H→L	0.66740
	$S_0 \rightarrow S_5$	2.28 eV (542.63 nm)	1.0127	H-2→L	0.66246
D4-T	$S_0 \rightarrow S_1$	1.66 eV (746.40 nm)	0.8033	H→L	0.67559
	$S_0 \rightarrow S_3$	2.26 eV (548.26 nm)	1.1524	H-1→L	0.68532
D5	$S_0 \rightarrow S_1$	1.63 eV (756.75 nm)	0.7133	H→L	0.70127
	$S_0 \rightarrow S_3$	2.40 eV (517.13 nm)	0.9948	H-2→L	0.68512
D5-T	$S_0 \rightarrow S_1$	1.59 eV (780.39 nm)	0.7311	H→L	0.70404
D6	$S_0 \rightarrow S_1$	1.78 eV (696.72 nm)	0.1668	H→L	0.50547
				H-1→L	0.38900
				H→L+1	0.22681
				H-1→L+1	0.20000
	$S_0 \rightarrow S_2$	1.89 eV (655.46 nm)	1.0518	H-1→L	0.50916
				H→L	0.42030
				H-1→L+1	0.20135
D6-T	$S_0 \rightarrow S_1$	1.85 eV (671.30 nm)	1.1699	H→L	0.67188
D7	$S_0 \rightarrow S_1$	1.53 eV (810.15 nm)	1.2761	H→L	0.69749
D7-T	$S_0 \rightarrow S_1$	1.50 eV (825.02 nm)	1.3053	H→L	0.70029
D8	$S_0 \rightarrow S_1$	1.41 eV (880.25 nm)	1.1144	H→L	0.66460
				H→L+1	0.23030
D8-T	$S_0 \rightarrow S_1$	1.38 eV (898.84 nm)	1.1128	H→L	0.68088
D9	$S_0 \rightarrow S_1$	1.39 eV (889.37 nm)	1.3075	H→L	0.65999
D9-T	$S_0 \rightarrow S_1$	1.37 eV (907.44 nm)	1.3221	H→L	0.67582
D1'	$S_0 \rightarrow S_1$	1.78 eV (694.83 nm)	2.1497	H→L	0.70656
D1'-T	$S_0 \rightarrow S_1$	1.77 eV (702.07 nm)	2.1762	H→L	0.70682
D2'	$S_0 \rightarrow S_1$	1.59 eV (782.11 nm)	2.3906	H→L	0.70605
D2'-T	$S_0 \rightarrow S_1$	1.56 eV (794.36 nm)	2.4018	H→L	0.70617
D3'	$S_0 \rightarrow S_1$	1.34 eV (925.70 nm)	2.4794	H→L	0.69879
D3'-T	$S_0 \rightarrow S_1$	1.31 eV (949.00 nm)	2.5567	H→L	0.69938
D4'	$S_0 \rightarrow S_1$	1.57 eV (789.25 nm)	2.8548	H→L	0.70579
D4'-T	$S_0 \rightarrow S_1$	1.55 eV (798.82 nm)	2.8636	H→L	0.70589
D5'	$S_0 \rightarrow S_1$	1.92 eV (645.23 nm)	0.0768	H-1→L	0.69220
	$S_0 \rightarrow S_2$	2.03 eV (610.27 nm)	0.5826	H→L	0.69558

D5'-T	$S_0 \rightarrow S_1$	1.98 eV (625.55 nm)	0.5506	H→L	0.70219
D6'	$S_0 \rightarrow S_1$	1.40 eV (883.12 nm)	3.1450	H→L	0.70490
D6'-T	$S_0 \rightarrow S_1$	1.38 eV (898.43 nm)	3.1557	H→L	0.70502
D7'	$S_0 \rightarrow S_1$	1.39 eV (890.92 nm)	3.4232	H→L	0.70216
D7'-T	$S_0 \rightarrow S_1$	1.36 eV (909.23 nm)	3.4281	H→L	0.70236

Table S2 Reproduced results of Probe1, BODIPY1, Probe2 and BODIPY2 in literature “Org. Biomol. Chem., 2011, 9, 3844–3853” and the calculated excited states of DAMBO and DAMBO-T in this study at TDDFT//B3LYP/6-31G(d) level.

Compounds	Electronic transitions	Excitation energy	f	Composition	CI
Probe1	$S_0 \rightarrow S_1$	1.84 eV (674.0 nm)	0.0004	H→L	0.7066
	$S_0 \rightarrow S_4$	2.96 eV (418.8 nm)	0.3694	H→L+2	0.4850
				H→L+1	0.2918
				H-1→L	0.2254
BODIPY1	$S_0 \rightarrow S_1$	3.02 eV (411.1 nm)	0.4707	H→L	0.5689
				H-1→L	0.1265
Probe2	$S_0 \rightarrow S_1$	1.47 eV (842.5 nm)	0.0000	H→L	0.7063
	$S_0 \rightarrow S_5$	3.03 eV (409.8 nm)	0.4614	H→L+2	0.5663
				H-1→L+2	0.1828
BODIPY2	$S_0 \rightarrow S_1$	3.03 eV (408.9 nm)	0.4711	H→L	0.5683
				H-2→L	0.1775
DAMBO	$S_0 \rightarrow S_1$	2.12 eV (584.4 nm)	0.0004	H→L	0.7044
	$S_0 \rightarrow S_4$	2.61 eV (474.2 nm)	0.8466	H-1→L	0.7043
DAMBO-T	$S_0 \rightarrow S_1$	2.60 eV (477.0 nm)	0.8534	H→L	0.7057

Table S3. Calculated excited states of Probe1, BODIPY1, Probe2 and BODIPY2 in literature “Org. Biomol. Chem., 2011, 9, 3844–3853” and molecules DAMBO and DAMBO-T in this study at TDDFT//CAM-B3LYP/6-31G(d) level.

Compounds	Electronic transitions	Excitation energy	f	Composition	CI
Probe1	$S_0 \rightarrow S_1$	2.95 eV (420.7 nm)	0.4662	H→L	0.6921
BODIPY1	$S_0 \rightarrow S_1$	3.00 eV (413.8 nm)	0.5329	H→L	0.6983
Probe2	$S_0 \rightarrow S_1$	3.01 eV (412.6 nm)	0.5283	H→L	0.6980
BODIPY2	$S_0 \rightarrow S_1$	3.01 eV (411.4 nm)	0.5362	H→L	0.6980
DAMBO	$S_0 \rightarrow S_1$	2.57 eV (482.5 nm)	0.8834	H→L	0.2795

DAMBO-T	$S_0 \rightarrow S_1$	2.55 eV (486.1 nm)	0.8886	$H \rightarrow L$	0.6433
				$H-1 \rightarrow L$	0.7016

Table S4. Calculated results for some kinds of experimental probes based on PET without dark state. All at TDDFT//B3LYP/6-31G(d) level.

Compound	Electronic transitions	Excitation energy	f	Composition	CI
HKGgreen-2 ^[a]	$S_0 \rightarrow S_1$	2.81 eV (441.8 nm)	0.4131	$H \rightarrow L$	0.5834
	$S_0 \rightarrow S_2$	2.94 eV (421.0 nm)	0.0011	$H-1 \rightarrow L$	0.6995
BOD-NHOH ^[b]	$S_0 \rightarrow S_1$	2.46 eV (503.0 nm)	0.6966	$H \rightarrow L$	0.7046
	$S_0 \rightarrow S_2$	2.93 eV (423.7 nm)	0.1231	$H-1 \rightarrow L$	0.6392
				$H-2 \rightarrow L$	0.2890
DANPBO-H ^[c]	$S_0 \rightarrow S_1$	2.37 eV (522.7 nm)	0.6587	$H \rightarrow L$	0.5956
	$S_0 \rightarrow S_2$	2.55 eV (485.3 nm)	0.2204	$H-1 \rightarrow L$	0.7012
DANPBO-CH ₃ ^[c]	$S_0 \rightarrow S_1$	2.41 eV (515.5 nm)	0.6842	$H \rightarrow L$	0.5920
	$S_0 \rightarrow S_2$	2.55 eV (485.5 nm)	0.0122	$H-1 \rightarrow L$	0.7025
5a ^[d]	$S_0 \rightarrow S_1$	2.32 eV (533.7 nm)	0.9429	$H \rightarrow L$	0.6010
	$S_0 \rightarrow S_2$	2.49 eV (498.1 nm)	0.3210	$H-1 \rightarrow L$	0.7048
ACa1 ^[e]	$S_0 \rightarrow S_1$	3.56 eV (348.3 nm)	0.1807	$H \rightarrow L$	0.5300
				$H-1 \rightarrow L$	0.4455
	$S_0 \rightarrow S_2$	3.56 eV (348.0 nm)	0.1687	$H-1 \rightarrow L$	0.5154
				$H \rightarrow L$	0.4633
DPPL1 ^[f]	$S_0 \rightarrow S_1$	2.30 eV (539.2 nm)	1.3592	$H \rightarrow L$	0.7000
	$S_0 \rightarrow S_2$	2.70 eV (459.7 nm)	0.0013	$H-1 \rightarrow L$	0.7008

[a] Z. N. Sun, H. L. Wang, F. Q. Liu, Y. Chen, P. Kwong, H. Tam and D. Yang, *Org. Lett.*, 2009, **11**, 1887–1890.

[b] R. Wang, F. B. Yu, P. Liu and L. X. Chen, *Chem. Commun.*, 2012, **48**, 5310–5312.

[c] H. X. Zhang, J. B. Chen, X. F. Guo, H. Wang and H. S. Zhang, *Anal. Chem.*, 2014, **86**, 3115–3123.

[d] T. Kowada, S. Yamaguchi and K. Ohe, *Org. Lett.*, 2010, **12**, 296–299.

[e] (1) H. M. Kim, B. R. Kim, J. H. Hong, J. S. Park, K. J. Lee and B. R. Cho, *Angew. Chem. Int. Ed.*, 2007, **46**, 7445–7448. (2) H. M. Kim, B. R. Kim, M. J. An, J. H. Hong, K. J. Lee and B. R. Cho, *Chem. Eur. J.*, 2008, **14**, 2075–2083.

[f] G. J. Zhang, H. Y. Li, S. M. Bi, L. F. Song, Y. X. Lu, L. Zhang, J. J. Yua and L. M. Wang, *Analyst*, 2013, **138**, 6163–6170.

Section S4 The validation of the PET mechanism for all NO probes in this study

The PET mechanism for all NO probes in this study has been detailedly verified by molecular orbital approach. As shown in **Fig.S3-Fig.S17**, the most of compounds show typical PET process which is in well agreement with the original intention of our design strategy.

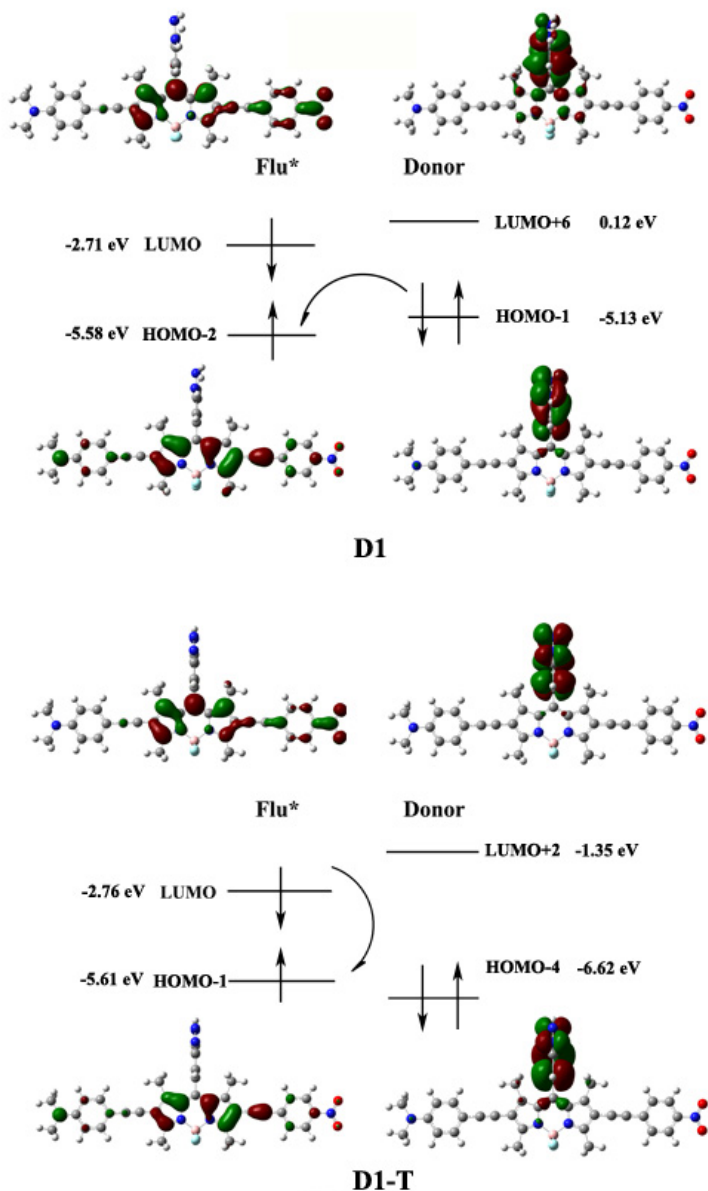


Fig.S3. The illustration of the PET process for D1 and D1-T.

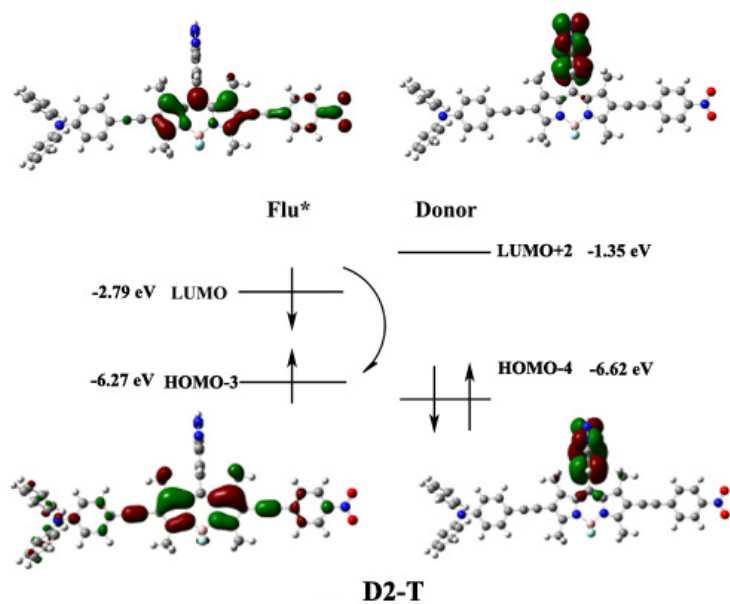
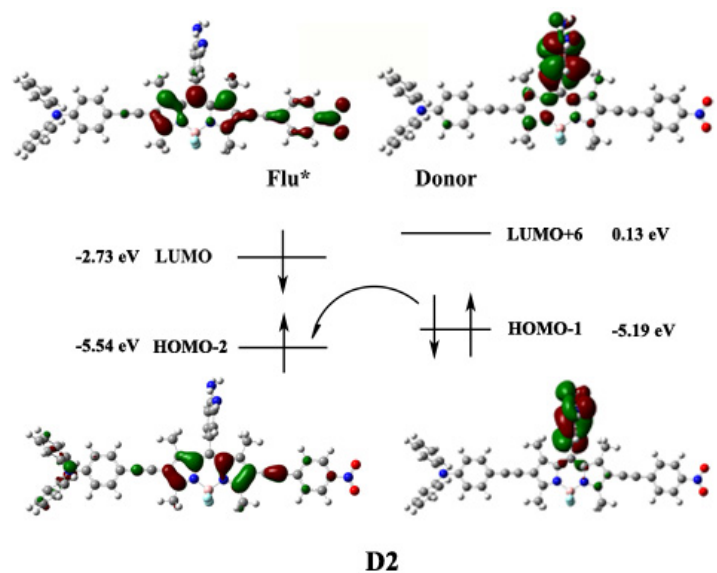


Fig.S4. The illustration of the PET process for D2 and D2-T.

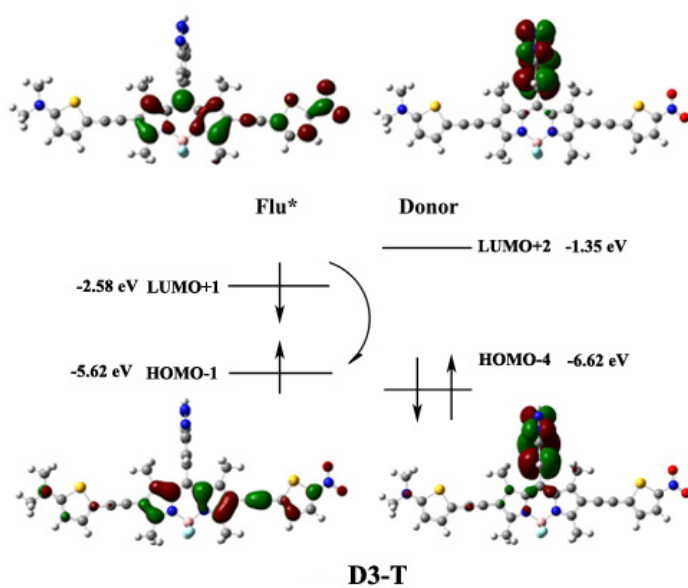
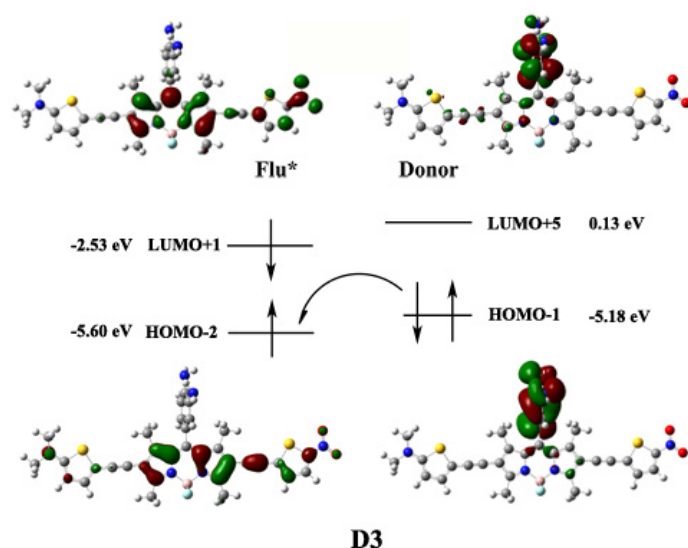


Fig.S5. The illustration of the PET process for D3 and D3-T.

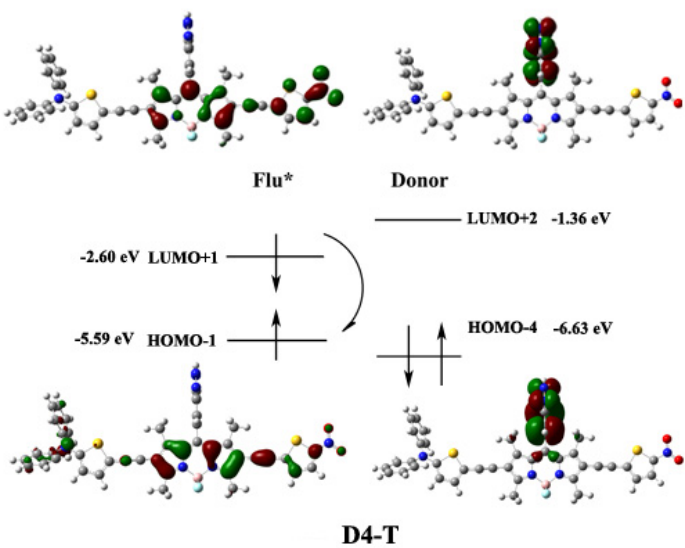
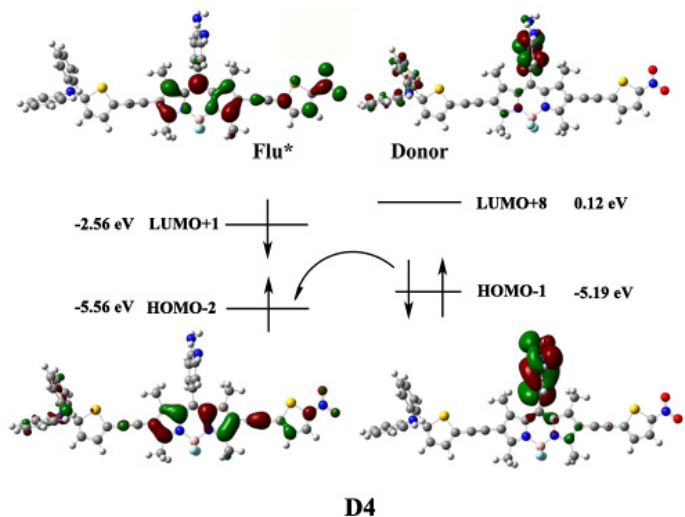


Fig.S6. The illustration of the PET process for D4 and D4-T.

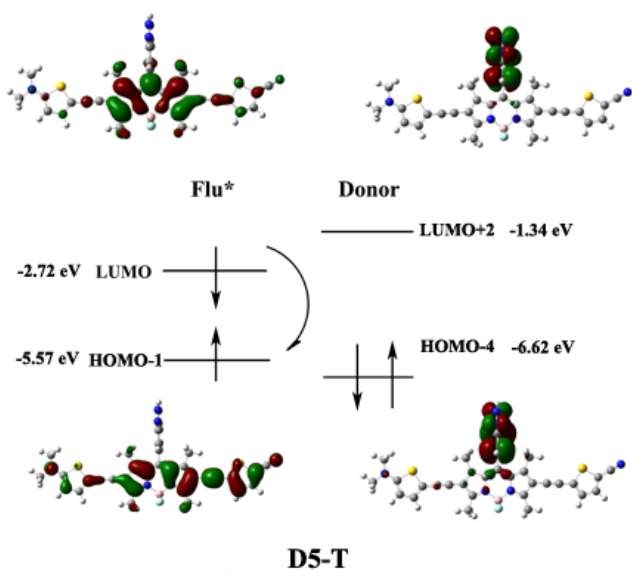
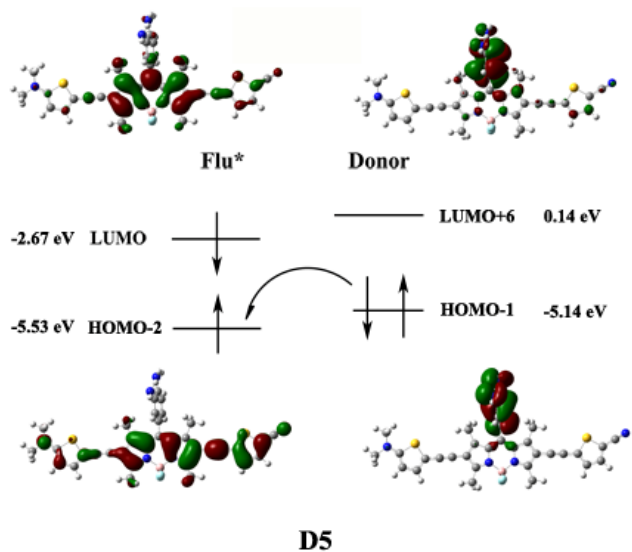


Fig.S7. The illustration of the PET process for D5 and D5-T.

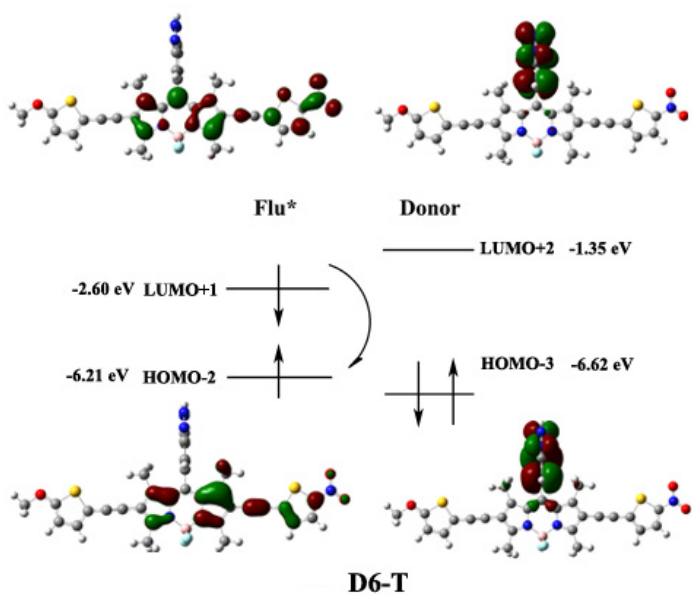
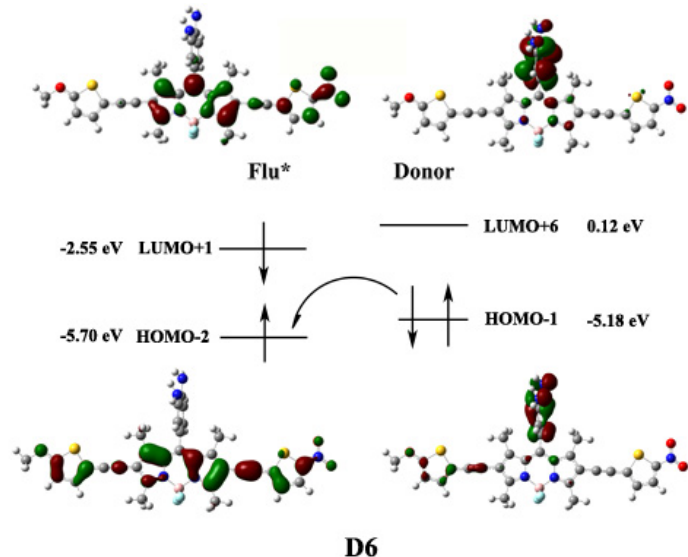


Fig.S8. The illustration of the PET process for D6 and D6-T.

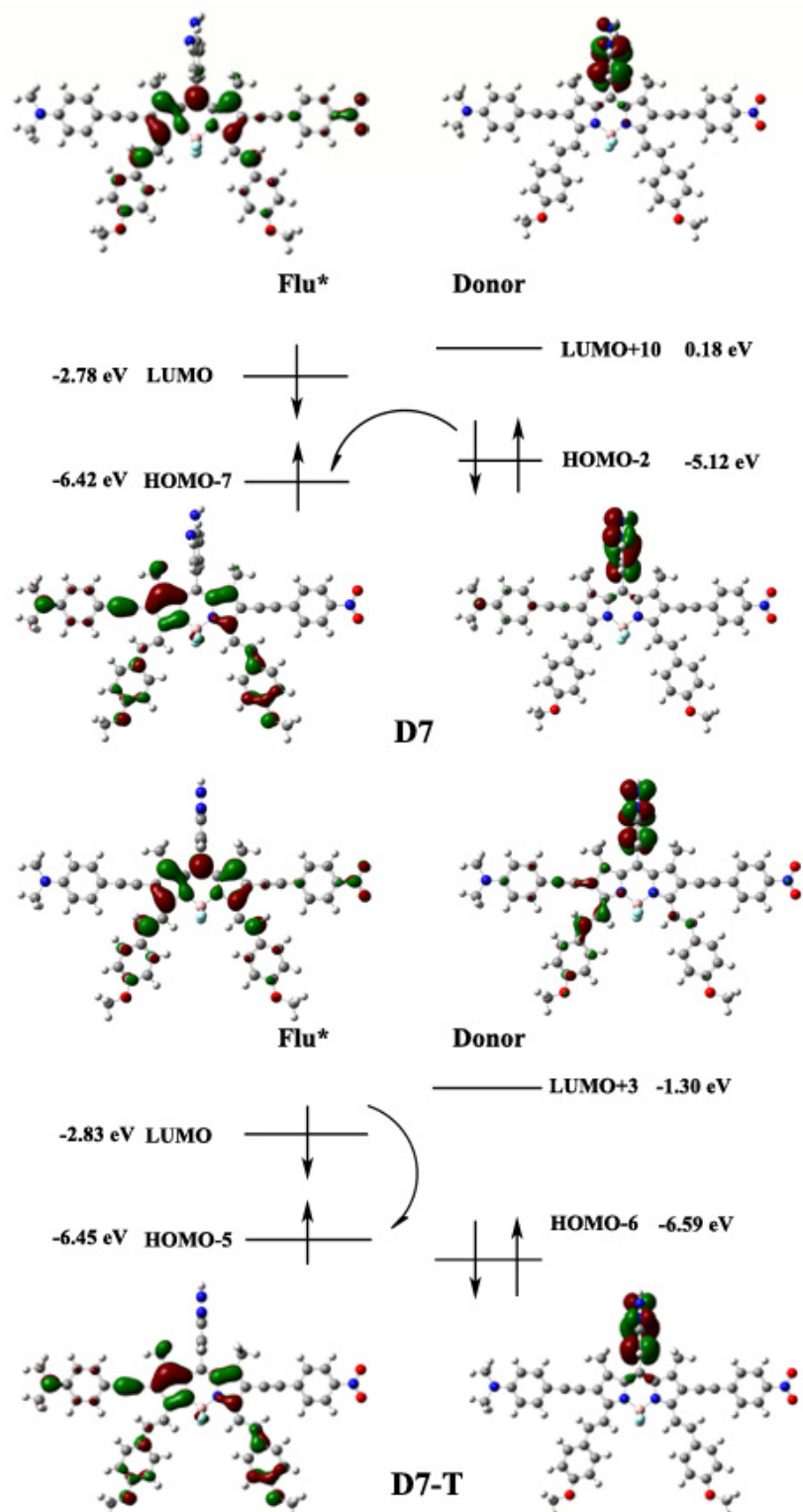


Fig.S9. The illustration of the PET process for D7 and D7-T.

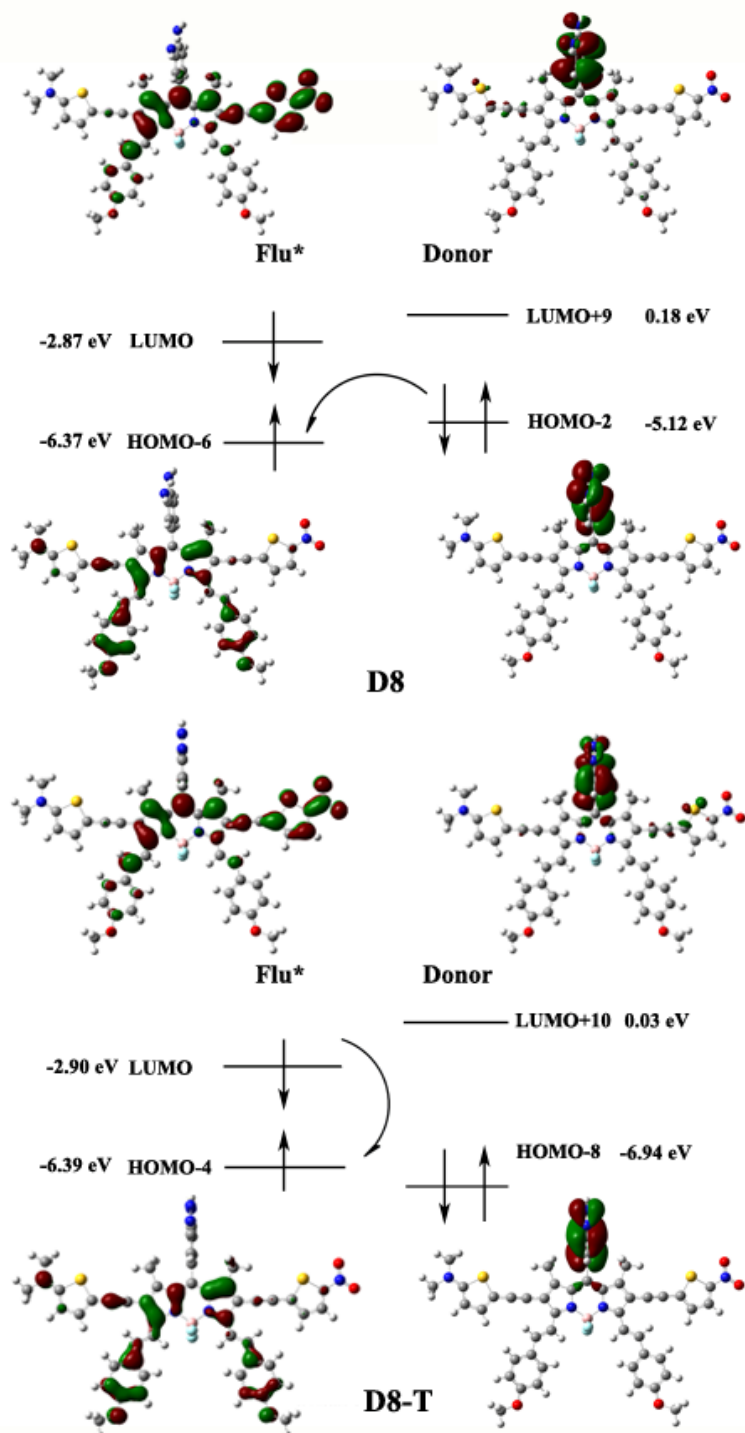


Fig.S10. The illustration of the PET process for D8 and D8-T.

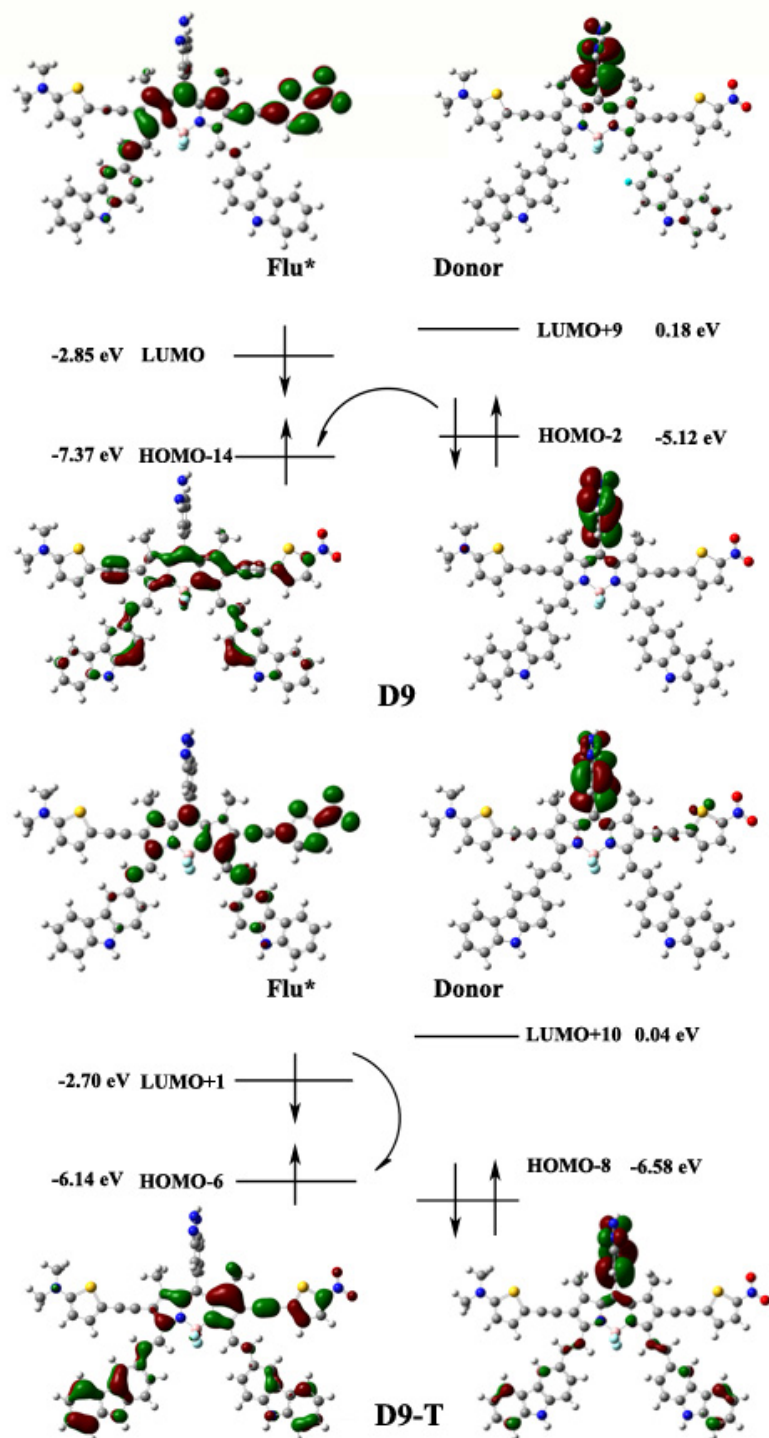


Fig.S11. The illustration of the PET process for D9 and D9-T.

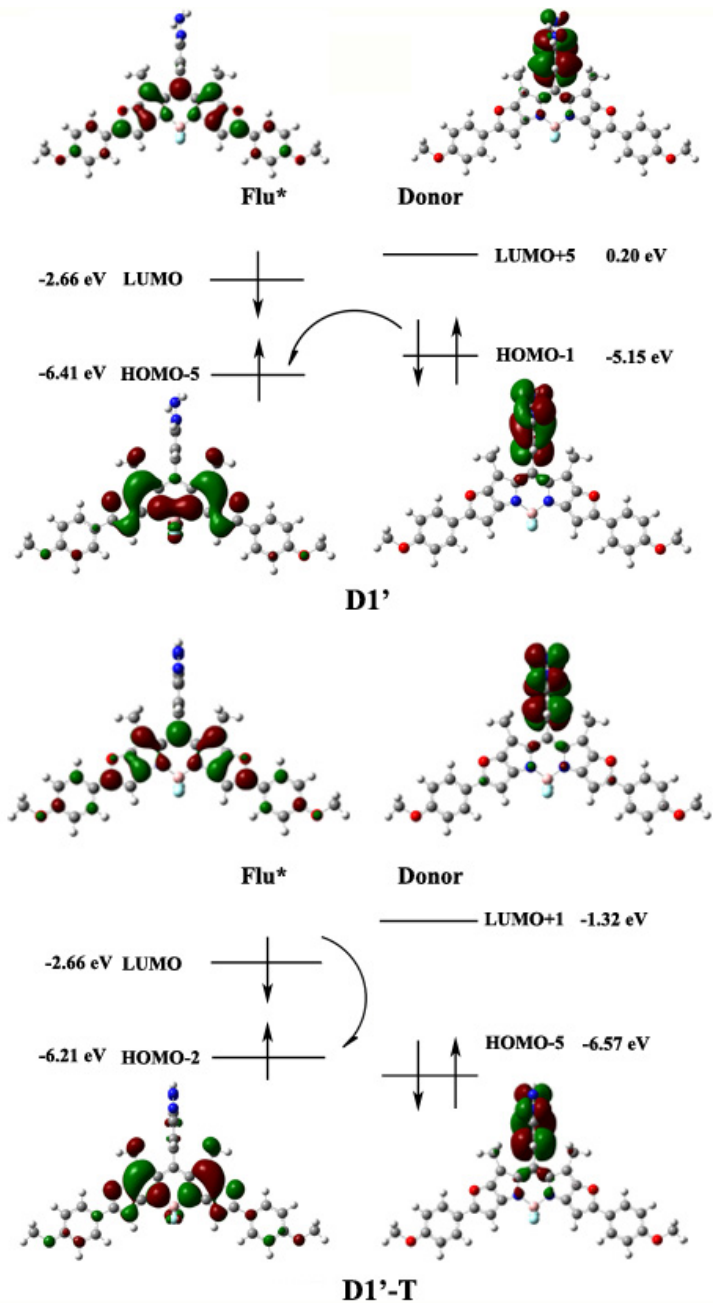


Fig.S12. The illustration of the PET process for D1' and D1'-T.

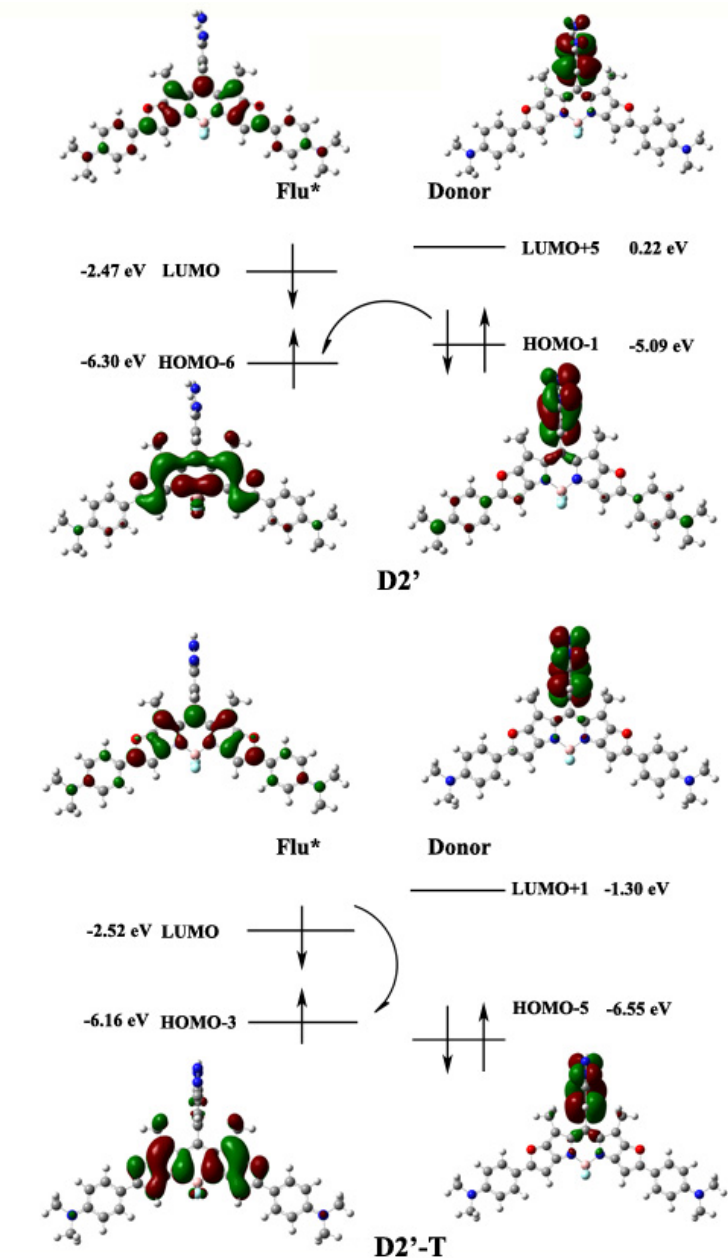


Fig.S13. The illustration of the PET process for $D2'$ and $D2'-T$.

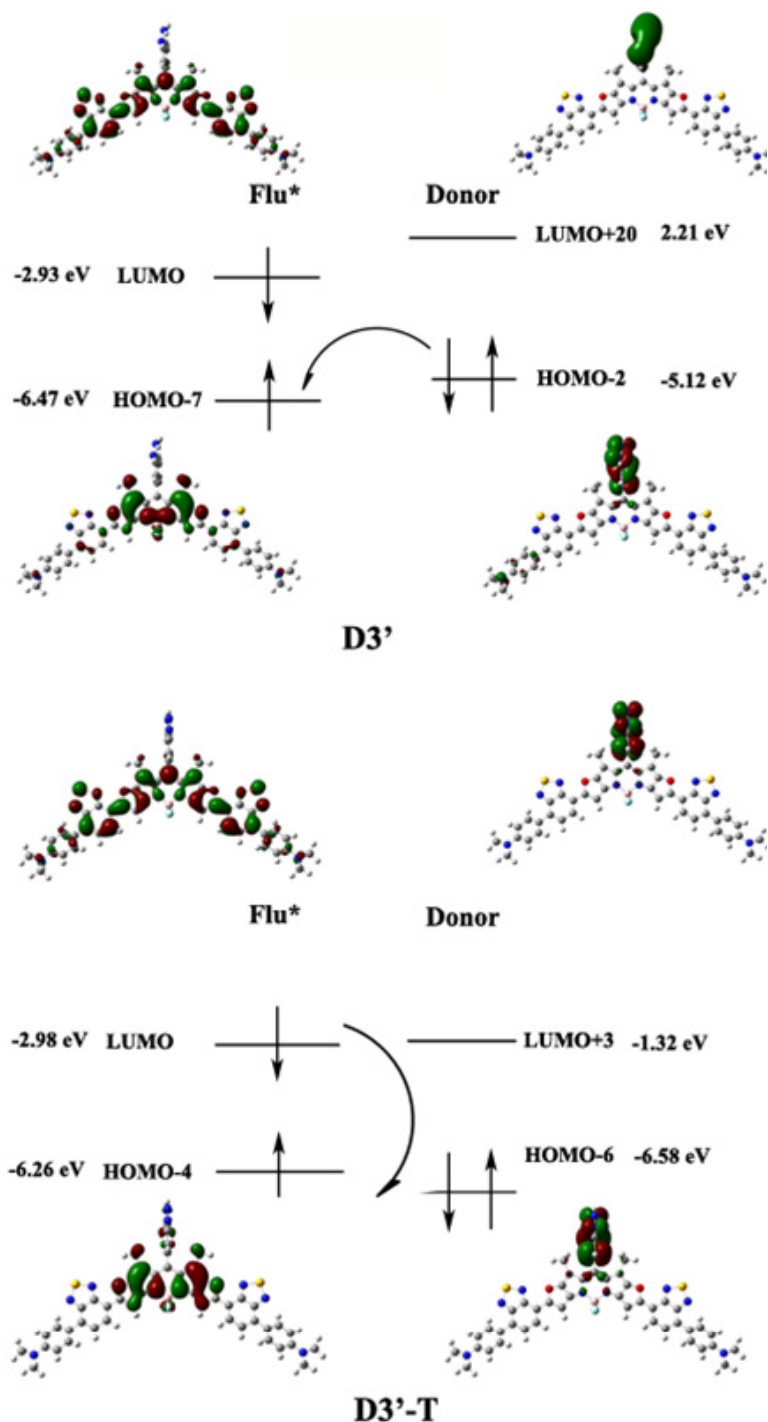


Fig.S13. The illustration of the non-PET process for D3' and D3'-T.

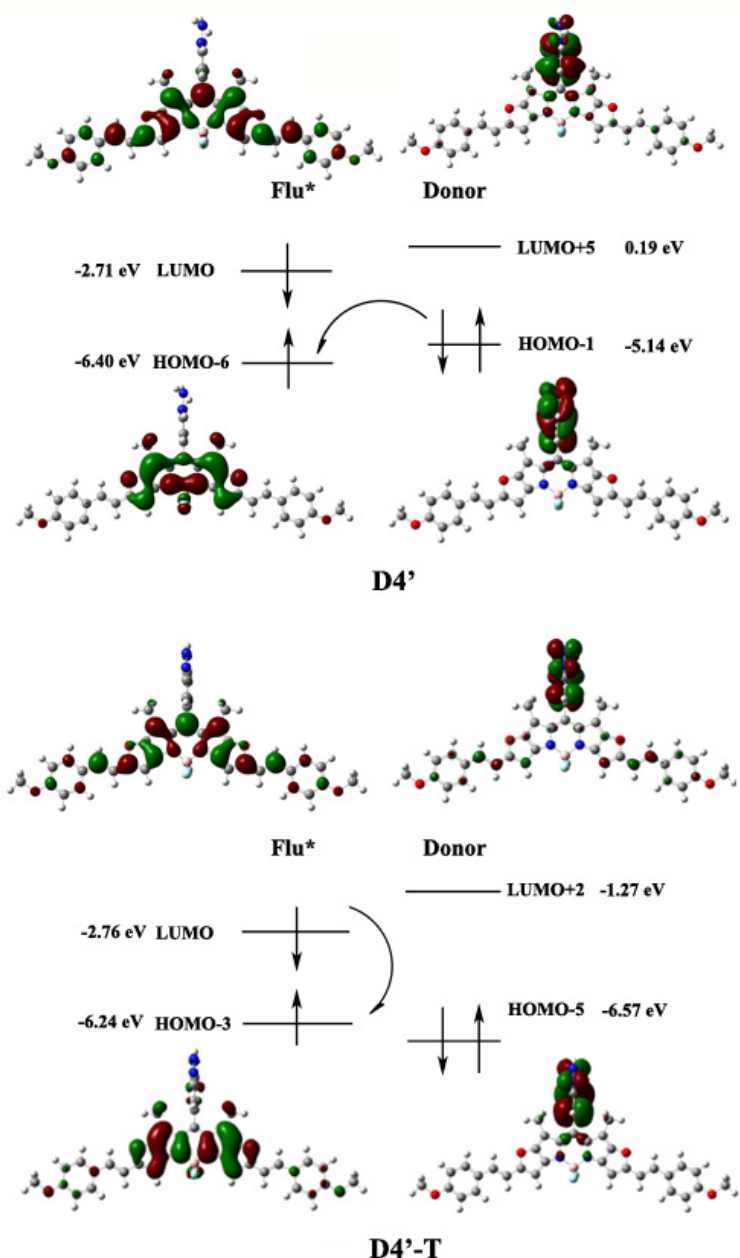


Fig.S14. The illustration of the PET process for D4' and D4'-T.

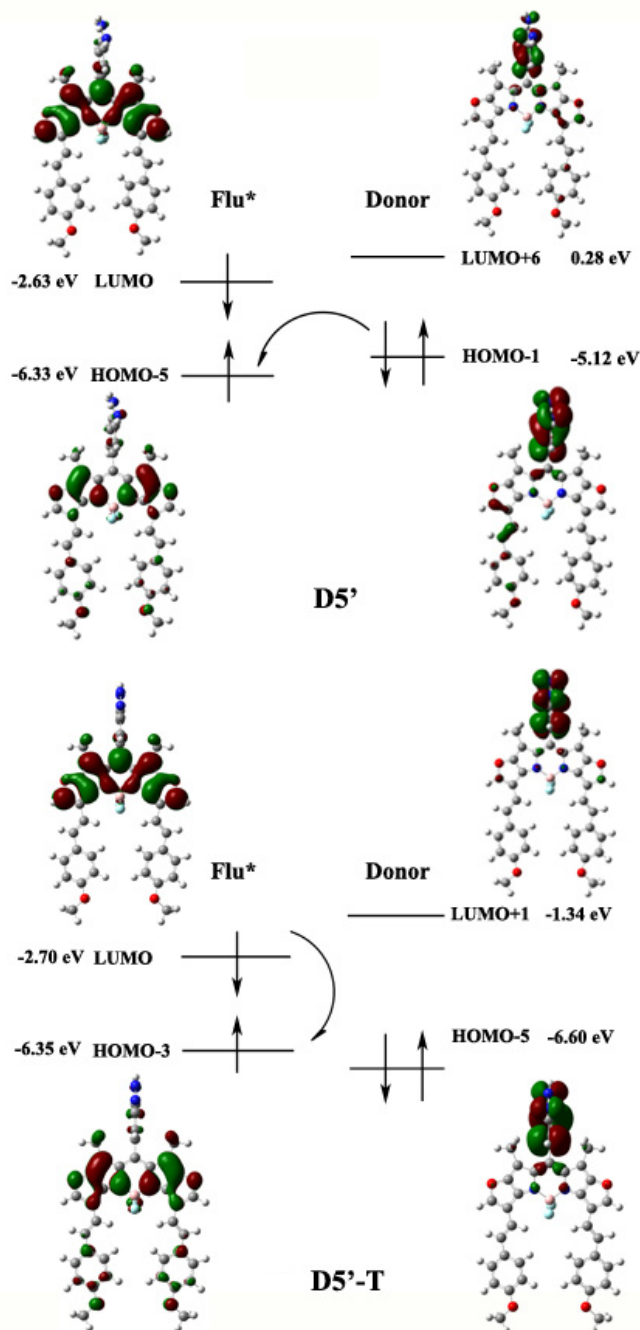


Fig.S15. The illustration of the PET process for D5' and D5'-T.

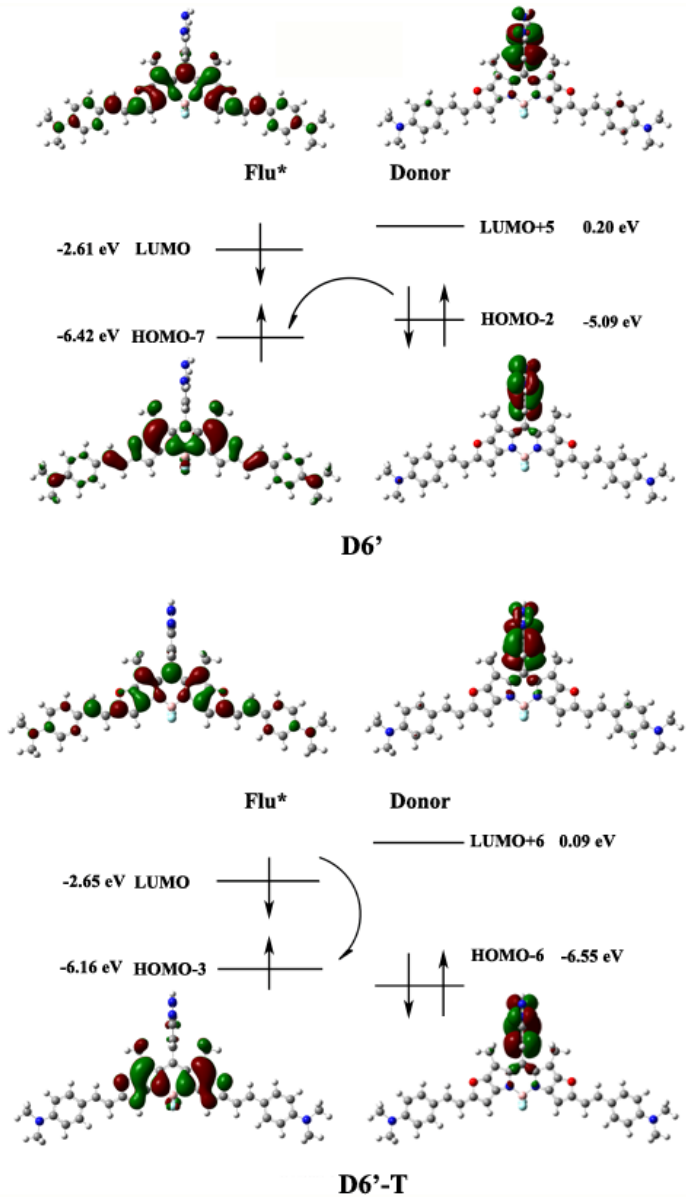


Fig.S16. The illustration of the PET process for D6' and D6'-T.

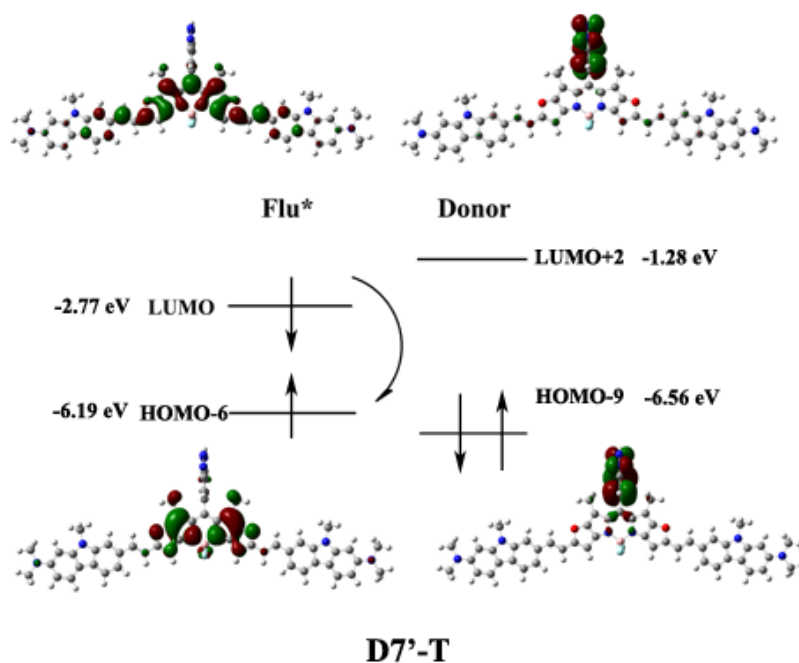
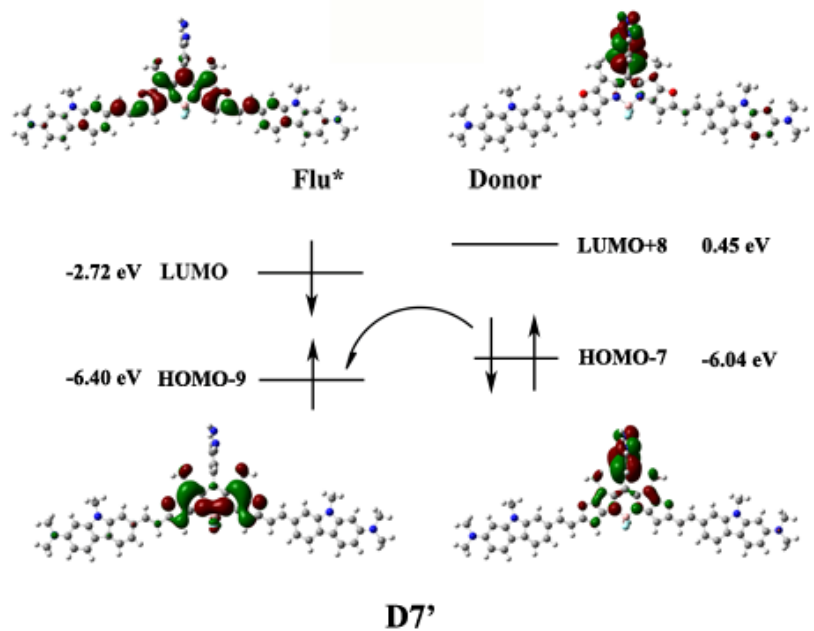


Fig.S17. The illustration of the PET process for D7' and D7'-T.